ON GRADIENT EFFECTIVE INDEX RAY-TRACING IN PLANAR LUNEBURG LENSES

by

GEBREDINGIL BERHE

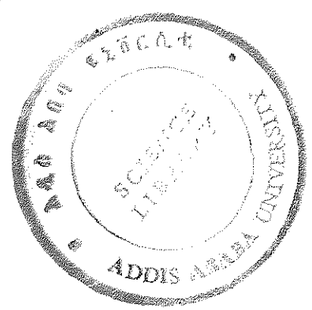

A Thesis

Presented to The

School of Graduate Studies

and

The Faculty of Science

Addis Ababa University

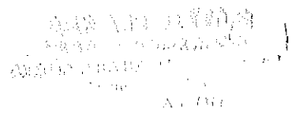

In Partial Fulfillment of the

Requirements for the Degree

Master of Science in Physics

June, 1988.

ACKNOWLEDGEMENT

I would like to express my deepest gratitude to my advisor and instructor Dr. D. A. Letov whose help and guidance made this paper a reality in a very short time. His rich experience in the field facilitated my progress in the work and aroused me to engage myself in further research activities in the field.

I am also grateful to W/o Letemeskal Asfaw and Gelana Amentie for their concern in bringing a book and articles from abroad.

Financial support of the Addis Ababa University is gratefully acknowledged.

Abstract

The problem adressed in the thesis lies in the field of integrated optics. For light propagation in dielectric waveguides interconnections are established between the dispersion equation, critical thickness and effective refractive index of the film, electric field distribution, power flow and a zig-zag model of propagation. All existing types of planar lenses are described and critically analyzed, among them the generalized Luneburg lenses seem to be one of the most advantageous for applications in integrated optical cricuits. Existing ray-tracing technique in such lenses is critically analyzed. A new ray-tracing approximation based on Fermat's principle is suggested. The procedure is successfully tested for a classical Luneburg lens in which case the integrals are taken analytically. Some detailed mathematical proofs have been relegated to the appendixes, which, however, should be regarded as integral parts of the paper.

Contents

INTRODUCTION

The interconnection of miniature optical components via optical waveguides on transparent dielectric substrates, using optical sources, modulators, detectors, filters, couplers, and other elements incorporated into circuits analogous to integrated electronic circuits for the execution of various communication, switching and logic functions is called integrated optics.

Since the frequency of light is some 10,000 times higher than the highest frequency of an electronic device, the amount of information that can be carried by a light signal is correspondingly greater. Moreover, opical circuits are in principle considerably faster than electronic circuits. Building even a simple integrated optical circuit, however, calls for techniques even more refined than the techniques employed for integrated electronic circuits.

The basic concept of integrated opical circuits is not new. Because of the obvious difficulties involved in realizing such devices, however, active research in the field was not begun until 1968. Even then no more than a dozen people at a few institutions were working on the problem (The institutions include Bell Laboratories, the University of Washington, the California Institute of Technology, the International Business Machines Corporation, Electronics Research Center Rockwell International. Since then the field has mushroomed. [1]

Nowadays application of optical integrated circuits extend from the real-time RF spectrum analyzer [2,3] capable of an instantaneous spectral analysis of an incoming radar beam, to monolithic

wavelength-multi plexed optical source [4] for terminal devices of fiber communication systems analog-to-digital converter [5] for the computer interfaces, and integrated lasers with modulators and detectors for digital computer memory devices[6].

Lens in integrated optics format constitute one of the basic passive elements for a number of application: collimating of the wave-guided light, coupling to fibers, carrying out Fourier transform functions.

The goal of the thesis.

The problem we address in this thesis lies in the field of integrated optics and is related to one type of planar lenses named after R.K. Luneburg. Particularly we are interested in ray tracing technique in such lenses. The development of a reliable accurate non-cumbursome method of ray tracing is needed for the estimation of possible fabrication tolerances which would not violate the achievement of the diffraction-limited potential of the planar Luneburg lens in integrated optical circuits. On the other hand the method helps to predict the expected focal spot size of the lens fabricated with a given tolerance. Or, vice versa it can assess the fabrication tolerance through measuring the actual focal spot size.

CHAPTER ONE

OPTICAL WAVEGUIDES THEORY AND PLANAR LENS DESIGN.

General Remarks

In general the simplest kind of transparent waveguide is obtained when a material with a higher refractive index is sandwitched between materials with a lower refractive index. In such a waveguide it is possible for a single light ray to zigzag back and forth through the inner layer, undergoing successive total internal reflections at both the upper and the lower interface. The only condition that must be met is that the angle of incidence of the light ray at both interfaces has to exceed the critical angle for total internal reflection. By embedding the light-conducting material on all sides in a material with a lower refractive index one can get an efficient channel waveguide. The cross-section of such a channel can be rectangular, as in the case of an actual thin-film waveguide, or circular as in the case of optical fiber.

A particular zigzag wave can be identified by the angle between the two legs of the zigzag. Waves with different angles propagate in the same film independently of one another. Thus each zigzag wave can be regarded as a separate waveguide mode.

Even though the light is totally reflected at the interfaces of such a waveguide, a small fraction of the propagating electromagnetic energy is always transmitted outside the guiding channel. Typically the intensity profile of the electromagnetic field is strongest at the center of the guiding channel and falls off gradually away from the center.

In a film of one micron thick a light wave typically bounces 1,000 times in order to propagate over a distance of one centimeter. If the surfaces of the film are not smooth, some of the light will be scattered each time the wave hits the upper or lower surface. The wave will not be able to propagate very far before all the light is scattered out of the film. In order to limit the light loss of a film to less than one decibel per centimeter the loss for each reflection must be less than one part in 10,000. That loss is a tenth the light loss for the better mirrors used in lasers. In spite of the progress made in the past few years most of the loss in thin-film waveguide is still due to the scattering of light. [8]

1.1. Zig-zag Model. The dispersion equation.

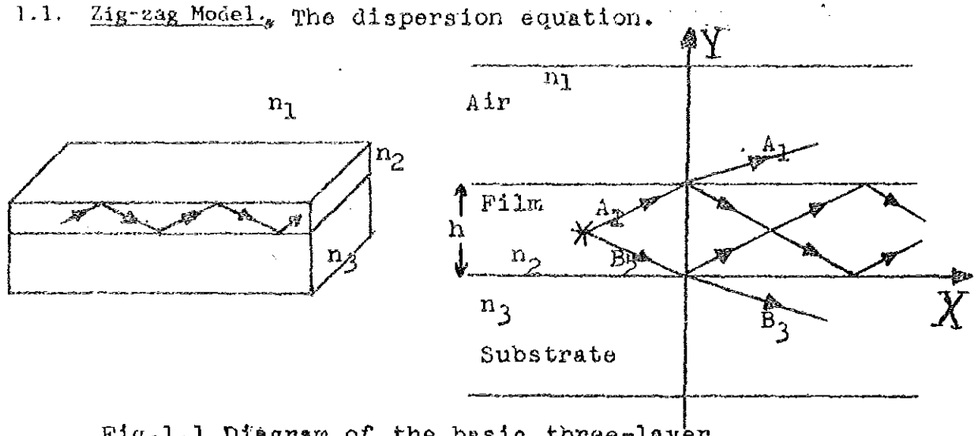

Fig.1.1 Diagram of the basic three-layer (single thin film) planar optical waveguide structure.

The structure shown in figure 1.1. is called an optical wave-guide. The thin film has a refractive index n_2 and a thickness h. It is placed between two media of refractive indices n_1 that of the surrounding medium, say air, and n_3 that of the substrate, where $n_1, n_3 < n_2$. Within this waveguide light rays are reflected through total internal reflection and follow a zig-zag path. Assuming that

a plane harmonic wave of transverse electric polarization E 0 E_z is propagating in the waveguide, the electric field distribution in the different media can be expressed by:

in the air $E_z^I = A_1 e^{ik_1^y Y}$ $h \leq y < +\infty$ --- (1.1)

in the waveguide $E_z^{II} = A_2 e^{ik_2^y Y} + B_2 e^{-ik_2^y Y}$ $0 \leq y \leq h$ --- (1.2)

in the Substrate $E_2^{III} = B_3 e^{-ik_3^y Y}$ $-\infty \leq y \leq 0$ ---(1.3)

where $\vec{k}_i = k_j^x + K_i^y$ ---------- (4)

$$K_i = K_o n_i , \quad K_o = \frac{2\pi}{\lambda_o}$$

$$K_i^2 = K_o^2 n_i^2 = (K_i^x)^2 + (K_i^y)^2 , \quad K_i^y = K_o^2 n_i^2 = K_x^2 \text{ --(1.5}$$

$$K_1^x \cdot X = K_2^x \cdot X = K_3^x \cdot X = K_x \cdot X \Longrightarrow K_1^x = K_2^x = K_3^x = K_x \text{--(1.6)}$$

λ_o - wavelength of light in vacuum.

The last statement follows from the require ment of matching the electromagnetic fields at any arbitrary point on the two interfaces of the waveguide. Propagation of the electric field along OX is describ by a factor $e^{i(K_x X - wt)}$ which is common for all three media and, for this reason, is omitted in all the intermediate formulas.

Taking the interface Y = h and applying the boundary condition that is the tangential components of the electric and magnetic fields are continuous as the boundary is crossed,

$$E_z^I = E_z^{II} \Longrightarrow A_1 e^{iK_1^y h} = A_2 e^{iK_2^y h} + B_2 e^{-iK_2^y h} \quad \text{--------(1.7)}$$

and $H_x^I = H_x^{II} \Longrightarrow K_1^y A_1 e^{iK^y h} = K_2^y A_2 e^{iK_2^y h} - K_2^y B_2 e^{-ik_2^y h}$ ---(1.8)

Substituting equ.(1.7)in (1.8),

$$K_1^y A_2 e^{iK_2^y h} + B_2 K^y e^{-ik^y h} = K_x^y A_2 e^{ik_2^y h} - K_2^y B_2 e^{-ik_2^y h}$$

$$\Longrightarrow \quad (k_1^y - K_2^y) e^{ik_2^y h} A_2 = -(K_1^y + K_2^y) e^{-ik_2^y h} B_2$$

$$\Longrightarrow \quad A_2 = \frac{(K_1^y + K_2^y)}{(K_2^y - K_1^y)} e^{-ik_2^y h} B_2 \text{ ----------(1.9)}$$

At the interface Y = 0

$$E_Z^{II} = E_Z^{III} \Longrightarrow A_2 + B_2 = B_3 \text{ ----------(1.10)}$$

and $H_X^{II} = H_X^{III} \Longrightarrow K_2^y A_2 - K_2^y B_2 = -K_3^y B_3$ ---------- (1.11)

Substituting equation (1.10)in (1.11)we have

$$K_2^y A_2 - K_2^y B_2 = -K_3^y A_2 - K_3^y B_2$$

If equation (1.9)is substituted in the above,

$$K_2^y \frac{(K_1^y + K_2^y)}{(K_2^y - K_1^y)} e^{-2iK_2^y h} B_2 - K_2^y B_2 = -K_3^y \frac{(K_1^y + K_2^y)}{(K_2^y - K_1^y)} e^{-2iK_2^y h} B_2 - K_3^y B_2$$

$$> (K_3^y - K_2^y) + (K_2^y + K_3^y) \frac{(K_1^y + K_2^y)}{(K_2^y - K_1^y)} e^{-i2k_2^y h} = 0$$

$$> e^{-2iK_2^y h} = \frac{(K_2^y - K_3^y)(K_2^y - K_1^y)}{(K_2^y + K_3^y)(K_2^y + K_1^y)} \qquad \text{----------(1.1.2)}$$

alternative way of derivation of equ.(1.12) is shown in appendix I.

Taking the natural logarithm of equation (1.12)

$$\ln e^{-2iK_2^y h} = \ln \left[\frac{(k_2^y - K_3^y)(K_2^y - K_1^y)}{(K_2^y + K_3^y)(K_2^y + K_1^y)} \right]$$

$$-2ik_2^y h = \ln \frac{(k_2^y - K_3^y)}{(K_2^y + K_3^y)} + \ln \frac{(k_2^y - K_1^y)}{(k_2^y + K_1^y)}$$

$$K_2^y h = \frac{1}{-2i} \ln \frac{(K_2^y - K_3^y)}{(K_2^y + K_3^y)} + \frac{1}{-2i} \ln \frac{(K_2^y - K_1^y)}{(k_2^y + K_1^y)}$$

$$K_2^y h = \frac{1}{2i} \ln \left(\frac{(K_2^y - K_3^y)}{(K_2^y + K_3^y)} \right)^{-1} + \frac{1}{2i} \ln \left(\frac{(K_2^y - K_1^y)}{(K_2^y + K_1^y)} \right)^{-1}$$

$$= \frac{1}{2i} \ln \frac{(K_2^y + K_3^y)}{(K_2^y - K_3^y)} + \frac{1}{2i} \ln \frac{(K_2^y + K_1^y)}{(K_2^y - K_1^y)}$$

From complex algebra if $Z = a + ib$, then

$$\arctan Z = \frac{1}{2i} \ln \frac{1 + iz}{1 - iz}$$

Implementation of the above formula imposes the following conditions upon K_1^y and K_3^y:

$K_1^y = iB_1$ - purely imaginary

$K_3^y = iB_3$ - imaginary number

Where $B_1 = \sqrt{K_x^2 - K_o^2 n_3^2}$ is real ----------(1.13)

$B_3 = \sqrt{K_x^2 - K_o^2 n_3^2}$ is real ----------(1.14)

$$\therefore K_2^y h = \frac{1}{2i} \ln \frac{K_2^y(1 + K_{3/K_2^y}^y)}{K_2^y (1-K_{3/K_2^y}^y)} + \frac{1}{2i} \ln \frac{K_2^y(1+ K_{1/K_2^y}^y)}{K_2^y (1-K_{1/K_2^y}^y)}$$

$$= \frac{1}{2i} \ln \frac{(1 + iB_{3/K_2^y})}{(1-iB_{3/K_2^y})} + \frac{1}{2i} \ln \frac{(1+ iB_{1/K_2^y})}{(1-iB_{1/K_2^y})}$$

$$= \frac{1}{2i} \ln \frac{(1+ iz_3)}{(1 - iz_3)} + \frac{1}{2i} \ln \frac{(1+iz_1)}{(1-iz_1)}$$

where $Z_1 = B_{1/K_2^y}$ and $Z_3 = B_{3/K_2^y}$

$$\therefore K_2^y h - \arctan \frac{B_3}{K_2^y} - \arctan \frac{B_1}{K_2^y} = m \pi \quad \text{----------(1.15a)}$$

The term $m\pi$ results from the periodic nature of the arctangent function.

Let's examine the physical sense of each term in equation (15 a). From the theory of reflection of a plane wave at the boundary n_2/n_1 of the two isotropic non-conducting media it is known [9] that the ratio B_1/K_2^y describes tangent of a half of the phase shift experienced by the totally reflected wave at this interface, that is

$$\text{reflected wave} = \text{incident wave} \cdot e^{-i\phi}$$

where $\tan \frac{\phi_1}{2} = B_1/K_2^y$ or $\frac{\phi_1}{2} = \arctan B_1/K_2^y$.

Similarly for the boundary n_2/n_3, we come to

$$\tan \frac{\phi_3}{2} = B_3/K_2^y \quad \text{or} \quad \frac{\phi_3}{2} = \arctan B_3/K_2^y$$

Multiplying equation (1.15a) by a factor of 2, we have the following expression.

$$2K_2^y h - 2 \arctan \frac{B_3}{K_2^y} - 2 \arctan B_1/K_2^y = 2m\pi \qquad (1.15b)$$

or $$2K_2^y h - \phi_3 - \phi_1 = 2\pi m \text{----------} (1.16)$$

The first term in equ. (1.16) describes the increase of the phase of the plane wave as it propagates forth and back along oy direction, making one complete cycle. Therefore equation (1.16) can be treated as the condition for a special standing optical wave in oy direction in the waveguide: The total phase change for one complete cycle of two subsequent reflections at points P and Q (see fig. 1.2) should be equal to the integer multiple of 2π.

	Point P		Point Q		Point R
	before reflection	after reflection	before reflection	after reflection	before reflection
Phase shift	0	$-\Phi_3$	$-\Phi_3 + K_2^y h$	$-\Phi_3 + K_2^y h - \Phi_1$	$-\Phi_3 + K_2^y h - \Phi_1 + K_2^y h$

One complete cycle or subsequent reflections

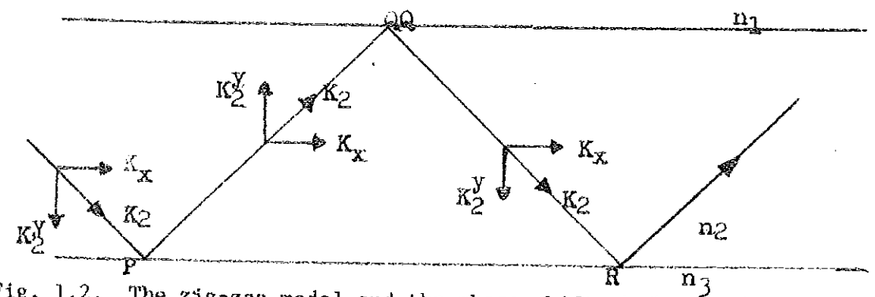

Fig. 1.2. The zig-zag model and the phase shifts before and after reflections at subsequent points P, Q, and R.

In bulk optics we know that the X-compenent of the wave vector $K_X = \frac{W}{U_X}$, U_X being the phase velocity

and $K_o = \frac{W}{C} = \frac{2\pi}{\lambda_o}$ C = speed of light in vacuum

W = anglar frequence of the source in vacuum

Dividing the first equation by the second, we get

$$\frac{K_x}{K_o} = \frac{C}{U_x}$$

Also for bulk light $n_1 = \frac{C}{U_1}$ ----------(*)

n_1 being the refractive index of medium 1.

Similar treatment in planar optics for a waveguided light in the film $\frac{Kx}{K_o} = \frac{C}{U_x} = \eta_{eff}$ ----------(**)

η_{eff} being the effective refractive index of the film.

Direct comparison of eq. (*) and (**) shows that the effective refractive index of the film η_{eff} in planar optics has the same physical sense as the bulk refractive index η in conventional bulk optics.

Substituting η_{eff} in equations (1.13) and (1.14)

$$B_1 = K_o\sqrt{n_{eff}^2 - n_1^2} \quad \text{----------(1.13')}$$

$$B_3 = K_o\sqrt{n_{eff}^2 - n_3^2} \quad \text{----------(1.14')}$$

Therefore expressing equation(1.15b)with these values substituted we have

$$2K_o\sqrt{n_2^2 - n_{eff}^2}\,h - 2\arctan\frac{\sqrt{n_{eff}^2 - n_3^2}}{\sqrt{n_2^2 - n_{eff}^2}} - 2\arctan\frac{\sqrt{n_{eff}^2 - n_1^2}}{\sqrt{n_2^2 - n_{eff}^2}} = 2m\pi$$

$$\Longrightarrow 2x\frac{2\pi}{\lambda_o}h\sqrt{n_2^2 - n_{eff}^2} = 2\arctan\frac{\sqrt{n_{eff}^2 - n_3^2}}{\sqrt{n_2^2 - n_{eff}^2}} \pm 2\arctan\frac{\sqrt{n_{eff}^2 - n_1^2}}{\sqrt{n_2^2 - n_{eff}^2}} \pm 2m\pi$$

$$\Longrightarrow \frac{h}{\lambda_o} = \frac{1}{2\pi\sqrt{n_2^2 - n_{eff}^2}}\left[\arctan\frac{\sqrt{n_{eff}^2 - n_3^2}}{\sqrt{n_2^2 - n_{eff}^2}} \pm \arctan\frac{\sqrt{n_2^2 - n_1^2}}{\sqrt{n_2^2 - n_{eff}^2}} \pm m\pi\right] \quad (1.17)$$

When $n_{eff} = n_3$, we get (h/λ) crit, a minimal critical value of this parameter.

$$\frac{(h)}{\lambda}\ crit = \frac{1}{2\pi\left(n_2^2 - n_{eff}^2\right)^{1/2}}\left[\arctan\ \frac{\left(n_{eff}^2 - n_1^2\right)^{1/2}}{\left(n_2^2 - n_{eff}^2\right)^{1/2}}\right] \quad \text{----------(1.18)}$$

If λ is given, from eq. (1.18) the minimal critical thickness of the film can be evaluated. The graph of eq. (1.17) for m=0,1,2 is shown in figure 1.3.

1.2 Field Distribution in the layers of the optical waveguide.

From equation (1.9)

$$B_2 = \frac{(K_2^y - K_1^y)}{(K_2^y + K_1^y)}\ e^{2iK_2^y h}\ A_2$$

Again from equn. (1.12)

$$\frac{(K_2^y - K_1^y)}{(K_2^y + K_1^y)}\ e^{2iK_2^y h} = \frac{K_2^y + K_3^y}{K_2^y - K_3^y}$$

$$\therefore \quad B_2 = \frac{K_2^y + K_3^y}{K_2^y - K_3^y}\ A_2 \quad \text{----------(1.19)}$$

Substituting this on equ. (1.2).

$$E_z = A_2 e^{iK_2^y y} + A_2\ \frac{(K_2^y + K_3^y)}{(K_2^y - K_3^y)}\ e^{-iK_2^y y}$$

$$E_z^{II} = A_2 \frac{(K_2^y - \beta_3)e^{iK_2^y y} \pm (K_2^y \pm i\beta_3)e^{-iK_2^y y})}{(K_2^y - i\beta_3)}$$

$$= \frac{2A_2}{(K_2^y - i\beta_3)} (K_2^2 \cos K_2^y y \pm \beta_3 \sin K_2^y y)$$

Multiplying by the complex conjugate

$$E_z^{II} = \frac{2A_2}{K_2^y - i\beta_3} \frac{(K_2^y \pm i\beta_3)}{(K_2^u \pm i\beta_3)} (K_2^y \cos K_2^y y \pm \beta_3 \sin K_2^y y)$$

$$= \frac{2A_2 K_2^y}{K_2^{y^2} \pm \beta_3^2} (K_2^y \cos K_2 y \pm \beta \sin K_2^y y) \pm \frac{i2A_2\beta_3}{K_2^{y^2} \pm \beta_3^2} (K_2^y \cos K^y y \pm \beta_3 \sin K_2$$

Taking the real part

$$\text{Re } E_z^{II}(y) = \frac{2A_2 k_2^y}{K_2^{y^2} \pm \beta_3^2} [K_2^y \cos K_2^y y \pm \beta_3 \sin K_2^y y] \text{ ----------(1.20a)}$$

Substituting the values of K_2^y and β_3, we have for the field distribution in the wave guide.

$$\text{Re } E_z^{II} (y) = \frac{2A_2\sqrt{n_2^2 - n_{eff}^2}}{K_o\sqrt{n_2^2 - n_3^2}} [K_o\sqrt{n_2^2 - m_{eff}^2} \cos (K_o\sqrt{n_2^2 - n_{eff}^2}y) \pm \beta_3 \sin(k_o\sqrt{n_2^2 - n_{eff}^2}y] \quad (1.20b)$$

Applying the boundary condition at the interface y=0

$$E_z^{III}(y) = E_z^{II}(y)$$

$$B_3 = A_2 \left[1 \pm \frac{K_2^y \pm iB_3}{K_2^y - iB_3}\right]$$

$$\therefore \quad E_z^{III}(y) = A_2\left[1 \pm \frac{K_2^y \pm iB_3}{K_2^y - iB_3}\right] e^{B_3 y}$$

Multiplying by the complex conjugate

$$E_z^{III}(y) = \frac{2A_2K_2^y e^{B_3 y}}{K_2^{y2} \pm B_3^2} \pm \frac{iB_3 2A_2K_2^y e^{B_3 y}}{K_2^{y2} \pm B_3^2} \qquad \text{---------- (1.21a)}$$

Taking the real part,

$$\text{Re } E_z^{III}(y) = \frac{2A_2(n_2^2 - n_{eff}^2)}{(n_2^2 - n_3^2)} e^{B_3 y} \qquad \text{---------- (1.21b)}$$

Again applying the boundary condition at the interface

y=h,

$$E_z^I = E_z^{II}$$

$$A_1 e^{-B_1 h} = A_2\left[e^{ik_2^y h} \pm \frac{(k_2^y \pm iB_3)}{(K_2^y - iB_3)} e^{-iK_2^y h}\right]$$

$$\Rightarrow A_1 = A_2 e^{B_1 h}\left[e^{iK_2^y h} \pm \frac{K_2^y \pm iB_3}{K_2^y - iB_3} e^{-iK_2^y h}\right]$$

Fig.1.4 Diagram of possible modes in planar single-film waveguide with $n_1=1.0$, $n_2=1.6$, $n_3=1.5$, at $\lambda=0.6328\mu m$

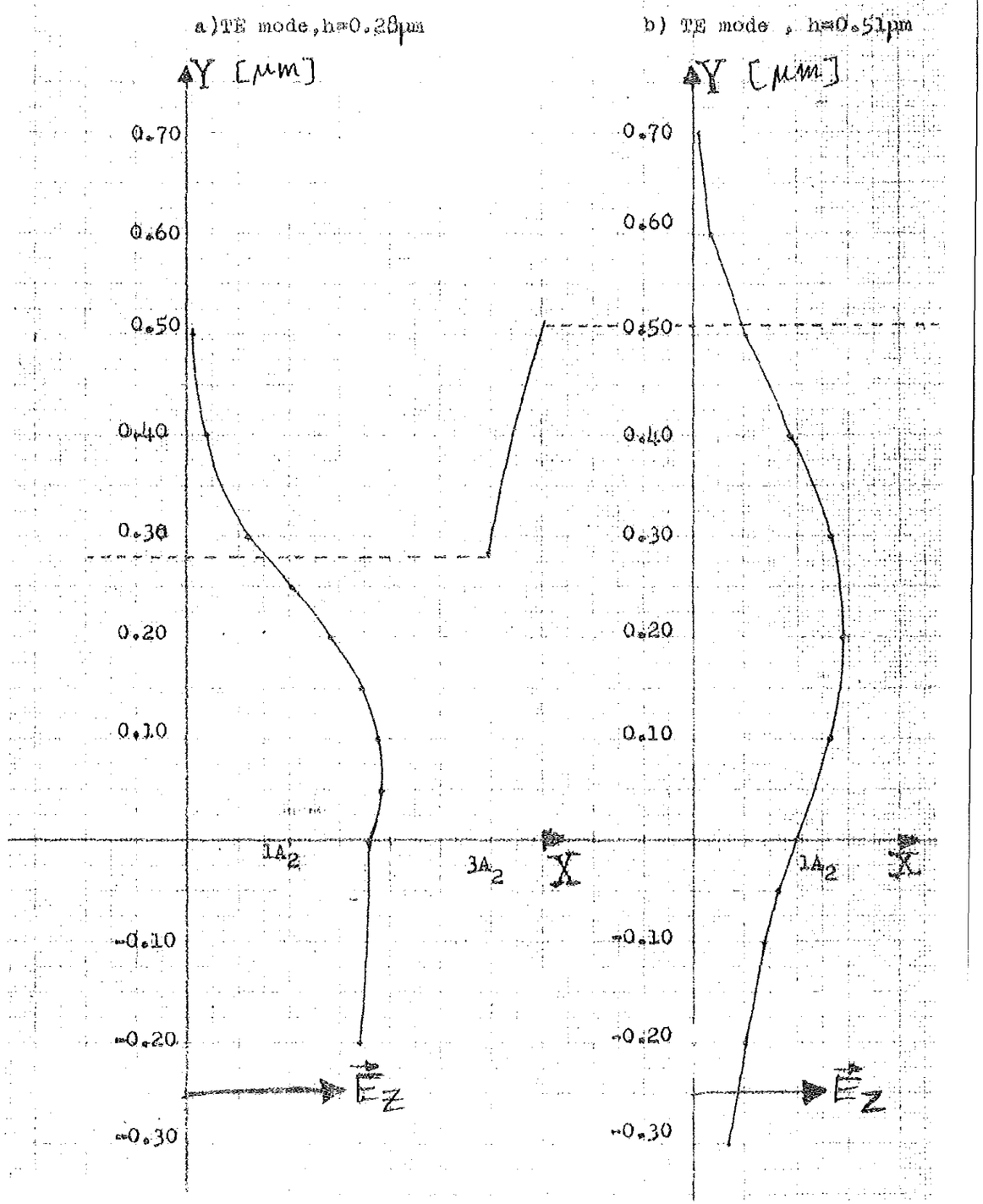

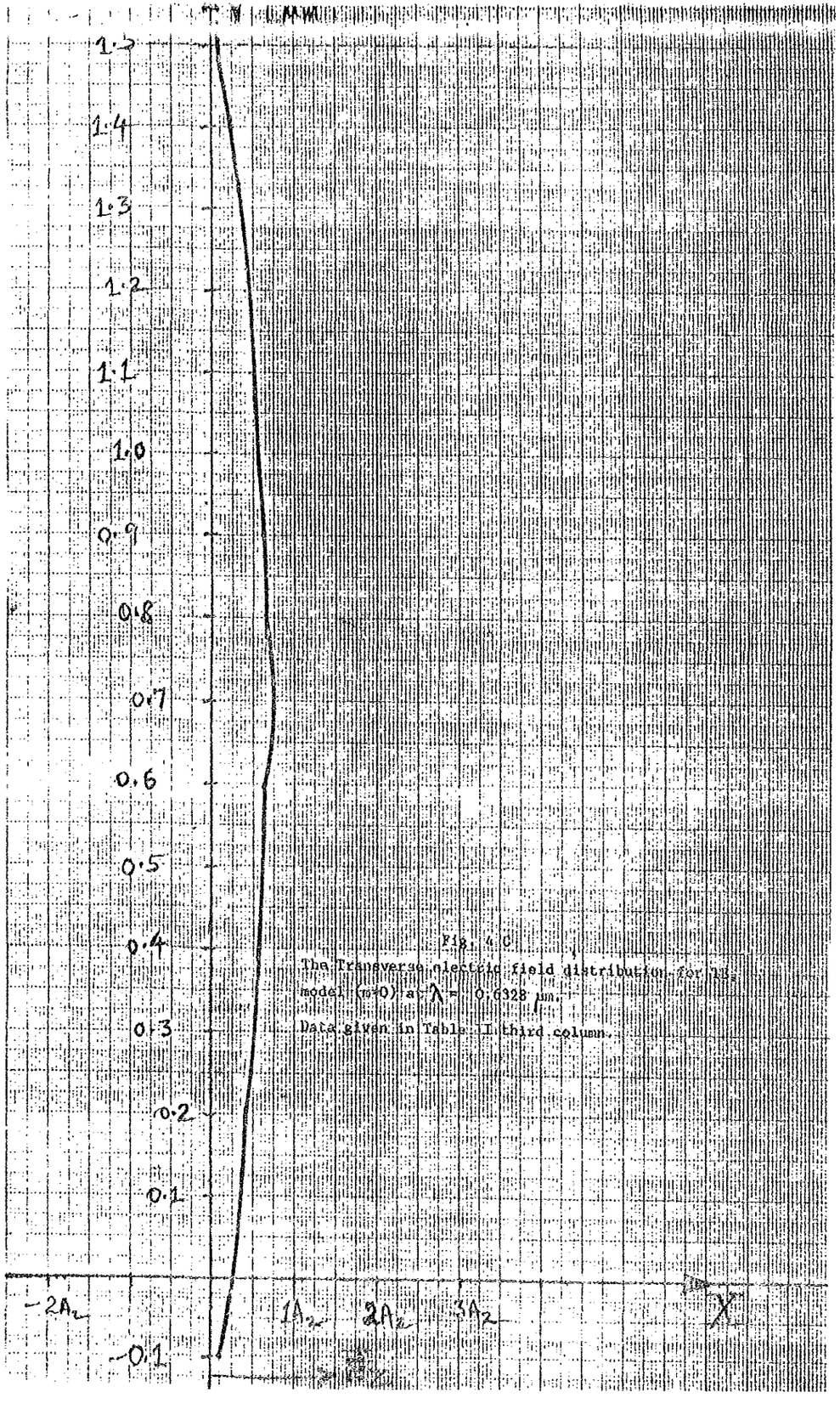

Fig. 4 C

The Transverse electric field distribution for HE_{12} model (m=0) at $\lambda = 0.6328$ μm.

Data given in Table II third column.

Table II The Transverse electric field distribution for TE_o model (m =0) at λ = 0.6328 μm.

m= 0
n_{eff}= 1.51
h/λ_o = 0.44
h = 0.28 μm.

y	$E_z^{III}(y)$
-5	$0.40A_2$
-2	$0.99A_2$
-1	$1.34A_2$
-0.5	$1.55A_2$
-0.2	$1.70A_2$
0	$1.81A_2$
0.05	$1.90A_2$
0.10	$1.86A_2$
0.10	$1.86A_2$
0.15	$1.69A_2$
0.20	$1.41A_2$
0.25	$1.03A_2$
0.275	$0.81A_2$
0.28	$0.76A_2$

m= 0
n_{eff}= 1.55
h/λ_o^o = 0.81
h= 0.51 μm

y	$E_z^{III}(y)$
-2.0	$0.0004A_2$
-1.0	$0.0206A_2$
-0.5	$0.145A_2$
-0.4	$0.21A_2$
-0.1	$0.69A_2$
-0.05	$0.84A_2$
0.0	$1.02A_2$
y	$E_z^{II}(y)$
0.0	$1.02A_2$
0.10	$1.324A_2$
0.10	$1.324A_2$
0.15	$1.40A_2$
0.20	$1.43A_2$
0.30	$1.31A_2$
0.40	$0.98A_2$
0.50	$0.51A_2$

m = 0
n_{eff} = 1.59
h/λ_o = 2.38
h = 1.50 μm.

y	$E_z^{III}(y)$
-0.3	$0.04A_2$
-0.2	$0.07A_2$
-0.1	$0.12A_2$
-0.05	$0.16A_2$
0	$0.21A_2$
y	$E_z^{II}(y)$
0	$0.21A_2$
0.2	$0.40A_2$
0.4	0.55
0.8	0.63
0.8	0.63
1.0	0.55
1.1	0.49
1.2	0.40
1.4	0.20
1.45	0.15

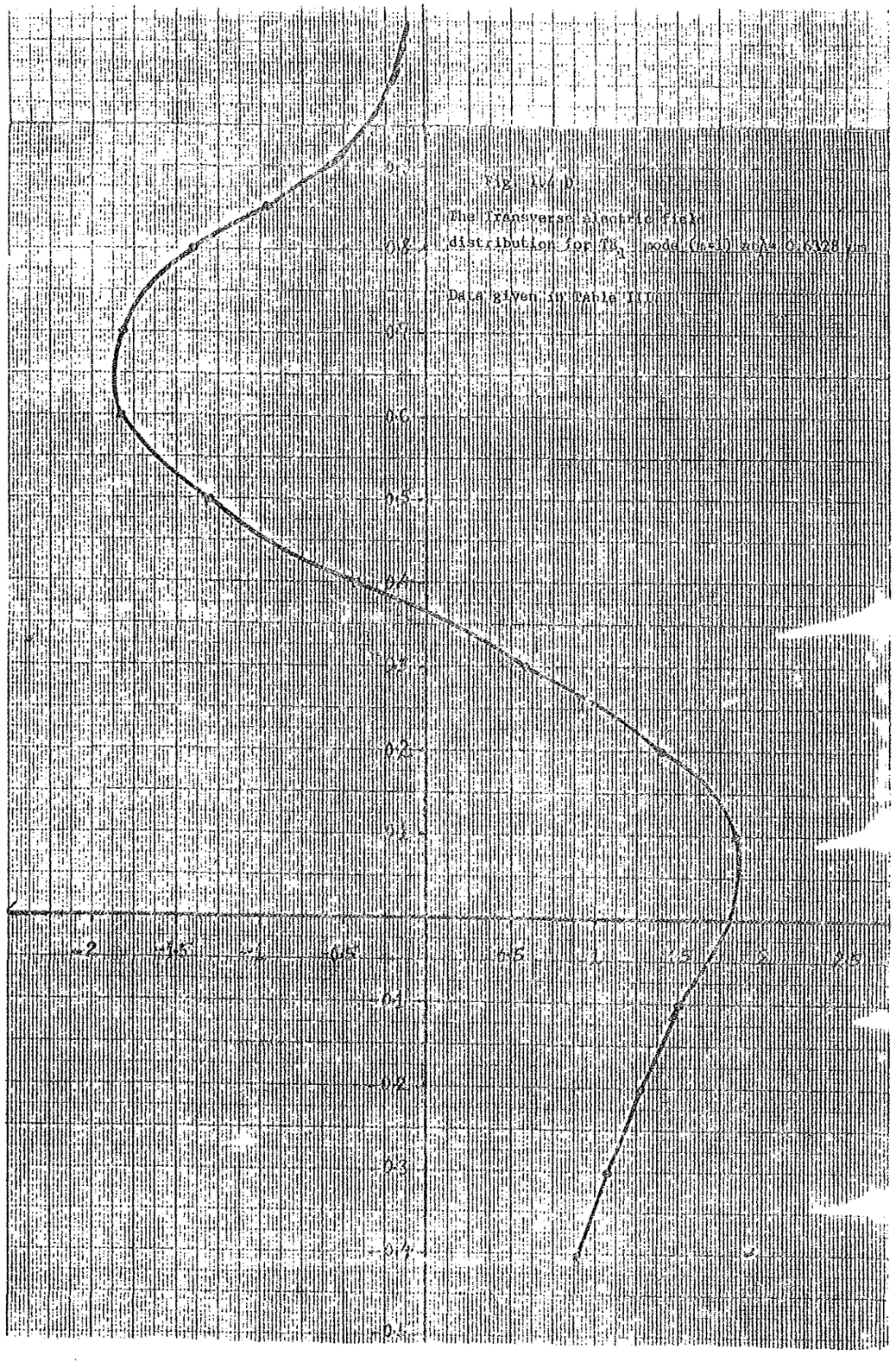

Fig. IV.D

The transverse electric field distribution for TE_{11} mode ($n=1$) at $\lambda = 0.8428\ \mu m$

Data given in Table III.

Table III The Transverse electric field distribution

for TE_1 mode (m=1) at = 0.6328 um

y	$E_z^{III}(y)$	y	$E_z^{II}(y)$	y	$E_z^{I}(y)$
-0.4	$0.90A_2$	0	$1.80A_2$	0.87	$-0.80A_2$
-0.3	$1.07A_2$	0.1	$1.86A_2$	0.90	-0.57
-0.2	$1.27A_2$	0.2	1.41	1.0	-0.19
-0.1	$1.51A_2$	0.3	0.59	1.5	-0.0007
0.0	$1.80A_2$	0.4	-0.42		
		0.5	-0.42		
		0.6	-1.83		
		0.8	-1.41		
		0.85	-0.98		
		0.87	-0.80		

$$\therefore \quad E_z^I(y) = A_2 \left(e^{iK_2^y h} \pm \frac{K_2^y \pm iB_3}{K_2^y - iB_3} e^{iK_2^y h}\right) e^{-iB_1(y-h)}$$

$$= \frac{2A_2K_2^y}{K_2^{y2} \pm B_3^2} \left(K_2^y \cos K_2^y h \pm B_3 \sin K_2^y h\right) e^{-B_1(y-h)} \quad \text{----(1.22)}$$

The graphs of $E_z(y)$ for different n_{eff} are plotted and shown in fig.1.4

The graphs show that a fraction of the propagating electric field is always transmitted outside the film. This fraction grows as $n_{eff} \Longrightarrow n_3$, that is when $h \Longrightarrow$ crit, if λ = constant.

1.3. Power Flow in the optical waveguide.

In a non-magnetic medium (i.e. $\mu = \mu_o$), the time average of the pointing vector $\vec{S}$ is

$\langle \vec{S} \rangle = \langle \vec{E} \times \vec{H} \rangle$ and we want to find the X component of the pointing vector $\langle S_x \rangle$

For T.E. case we get

$$\vec{E} \times \vec{H} = \begin{vmatrix} \hat{i} & \hat{j} & \hat{k} \\ o & o & E_z \\ H_x & h_y & 0 \end{vmatrix} = -E_z H_y \hat{i} \pm E_z H_x \hat{j}$$

Taking the magnitude only

$$\langle S_x \rangle = \tfrac{1}{2} \langle -E_z \cdot H_y \rangle$$

To find the y-component of $\vec{H}$, from Maxwell's equation

$$\vec{\nabla} \times \vec{E} = -\mu_o \frac{\partial \vec{H}}{\partial t}$$

Fig.1.3 Effective refractive index n_{eff} and phase velocity u_x of the waveguided light versus normalized thickness h/λ_0 for single - film asymmetric structure with $n_1=1.0$, $n_2=1.6$, $n_3=1.5$.

ξ =range of h/ values for single mode operation.

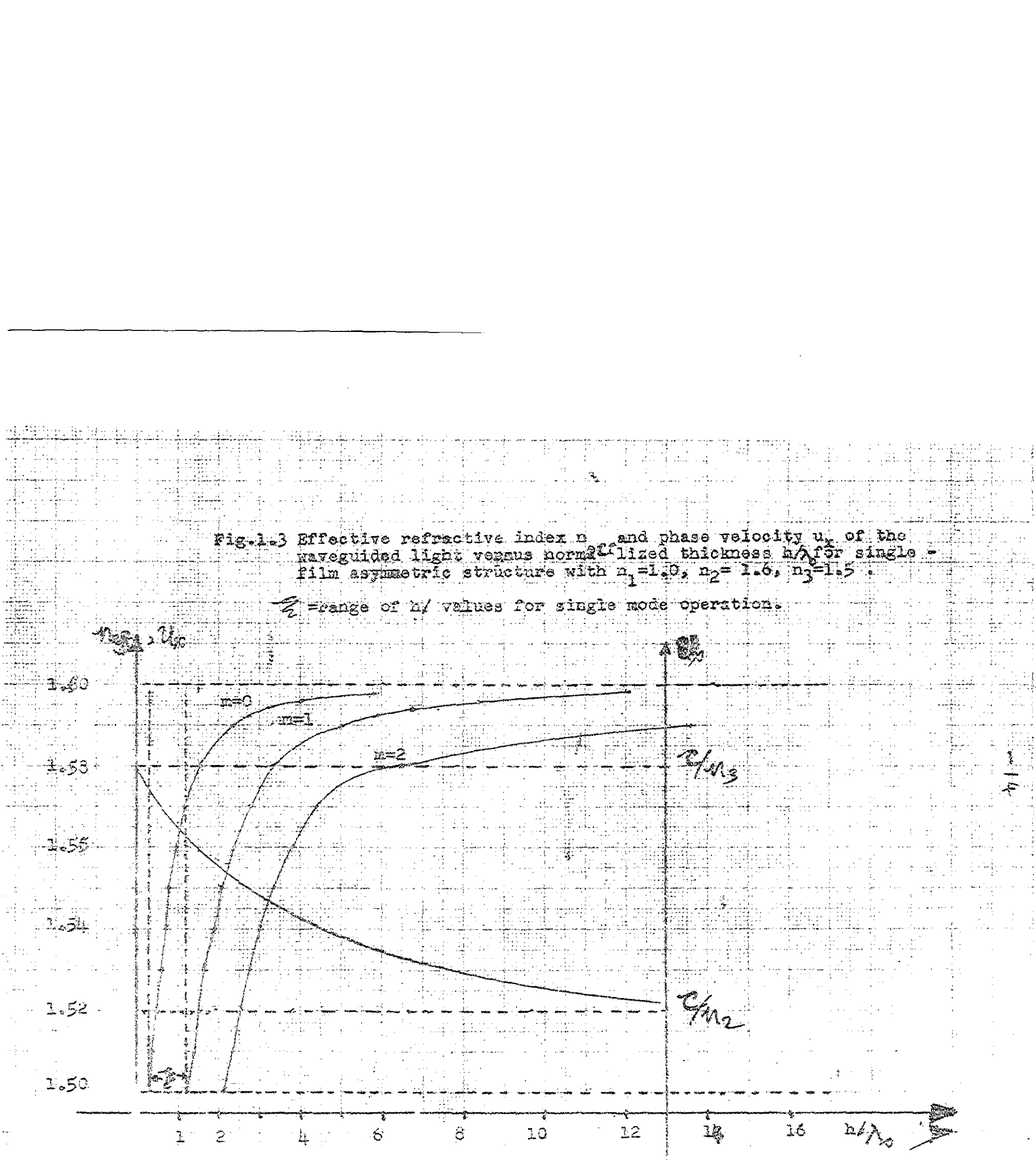

Table I

Effective model index as function of h/λ_0 for m=0,1,2.

n_{eff}	h/λ_0 m=0	M=1	m=2
1.50	0.32	1.21	2.11
1.51	0.44	1.38	2.33
1.52	0.52	1.52	2.52
1.53	0.60	1.67	2.73
1.54	0.70	1.85	3.00
1.55	0.81	2.07	3.33
1.56	1.00	2.37	3.78
1.57	1.19	2.81	4.43
1.58	1.56	3.54	4.42
1.59	2.38	5.18	13.58
1.592	2.71	5.84	
1.594	3.20	6.81	
1.596	4.01	8.43	
1.598	4.84	12.09	
1.5982	6.18	12.77	
1.5984	6.58	13.56	
1.5986	7.06	14.53	

Since $\vec{E}$ and $\vec{H}$ are proportional to $e^{i(\vec{K}\cdot\vec{r}-wt)}$

$\frac{\partial}{\partial t} = -iw$, and $\vec{\nabla} = i\vec{K}$.

$\therefore \quad i\vec{K} \times \vec{E} = -\mu_o(-iw)H \quad ; \quad \vec{K} \times \vec{E} = \begin{vmatrix} \hat{i} & \hat{j} & \hat{k} \\ k_x & k_y & o \\ o & o & E_z \end{vmatrix}$

Since it is a plane wave propagating in XOY plane, $k_z = 0$

$\therefore \quad \vec{K} \times \vec{E} = K_y E_z \hat{i} - K_x E_z \hat{j} = \mu_o w (H_z \hat{i} + H_y \hat{j})$

$$\Longrightarrow \quad H_y = \frac{-K_x E_z}{\mu_o w}$$

Hence $< S_x > = \frac{1}{2} < -E_z \cdot H_y >$

$$= \frac{K_x}{2\mu_o w} < E_z E_z^* > \text{ in general} \quad \text{--- (1.23)}$$

The time factor is cancelled when the complex conjugate is taken so the average is independent of time.

$$< S > = \frac{1K_x}{2\mu_o w} E_z E_z^* \quad \text{---------- (1.24)}$$

Equ. 1.24 decribes power flow in OX direction at a specified Y-coordinate.

1.31. Power in the thin film.

$$<S_x^{II}> = \frac{\frac{1}{2}K_x}{\mu_o \omega} E_z^{II} E_z^{II*}$$

$$= \frac{k_x}{\mu_o w} A_2 A_2^* \left(e^{iK_2^y y} + \frac{K_x^2 + iB_3}{K_2^2 - B_3} e^{-iK_2^y y}\right) \cdot \left(e^{-iK_2^y y} + \frac{K_2^y - iB_3}{K_2^y + iB_3} e^{iK_2^y y}\right)$$

$$= \frac{K_x A_2 A_2^*}{\mu_o w 2} \left[1 + 1 + \frac{K_2^y - iB_3}{K_2^y + iB_3} e^{2iK_2^y y} + \frac{K_2^y - iB_3}{K_2^y - iB_3} e^{-2iK_2^y y} \right] \quad \text{----(1.25)}$$

In order to calculate the integral power flow in the film let's integrate equ. (1.25)

$$P^{II} = \int_0^h \langle S_x^{II}(y) \rangle \, dy.$$

$$= \frac{K_x A_2 A_2^*}{2\mu_o w} \left[\int_0^h 2 \, dy + \int_0^h \mathrm{Re}\, 2iK_2^y y \, dy + \int_0^h \frac{1}{R} e^{-i2K_2^y y} \, dy \right]$$

Where $R = \dfrac{K_2^y - iB_3}{K_2^y + iB_3}$

$$= \frac{K_x A_2 A_2^*}{2\mu_o w} \left[2h + R \frac{1}{2iK_2^y} e^{2iK_2^y y} \Big|_{y=0}^{y=h} + \frac{1}{R} \frac{1}{-2iK_2^y} e^{-2iK_2^y y} \Big|_{y=0}^{y=h} \right]$$

$$= \frac{K_x A_2 A_2^*}{2\mu_o w} \left[2h + \frac{R}{2iK_2^y} (e^{2iK_2^y h} - 1) - \frac{1}{R 2iK_2^y} (e^{-2iK_2^y h} - 1) \right]$$

$$= \frac{K_x A_2 A_2^2}{2\mu_o w} \left[2h + \frac{1}{2iK_2^y} \left(\frac{4K_2^y k_1^y}{K_2^{y2} - k_1^{y2}} + \frac{4iK_2^y B_3}{K_2^{y2} + B_3^2} \right) \right.$$

$$P^{II} = \frac{K_x A_2 A_2^*}{\mu_o w \cdot 2} \left[2h + \frac{2B_1}{K_2^{y2} + B_1^2} + \frac{2B_3}{K_2^{y2} + B_3^2} \right]$$

$$\Longrightarrow \frac{K_x A_2 A_2^*}{\mu_o w} \left[h + \frac{B_1}{K_o^2 (n_2^2 - n_1^2)} + \frac{B_3}{K_o^2 (n_2^2 - n_3^2)} \right] \quad \text{---- (1.26)}$$

13.2 Power flow in the Substrate.

From equation (21 b), the expression for $E_z^{III}(y)$ is

$$E_z^{III}(y) = A_2 \left[1 + \frac{K_2^y + iB_3}{K_2^y - iB_3}\right] e^{B_3 y}$$

and $< S_x^{III} > = \frac{K_x A_2}{\mu_o w 2}\left[1+ \frac{K_2^y + iB_3}{B_2^y - iB_3}\right] e^{B_3 y} A_2^* \left(1 + \frac{K_2^y - iB_3}{K_2^y + iB_3}\right) e^{B_3 y}$

$$= \frac{K_x A_2 A_2^*}{\mu_o w 2} e^{2B_3 y} \left[1+1+\frac{K_2^y+iB_3}{K_2^y-iB^3} + \frac{K_2^y-iB_3}{K_2^y + iB_3}\right]$$

$$= \frac{K_x A_2 A_2^*}{\mu_o w 2} e^{2B_3 y} \left[2 + \frac{2K_2^{y2} - 2B_3^2}{K_2^{y2} + B_3^2}\right]$$

$$= \frac{K_x K_2^{y2} A_2 A_2^* e^{2B_3 y}}{\mu_o w K_2^{y2} + B_3^2} \qquad \text{----------(1.27)}$$

Integration through the substrate gives

$$P^{III} = \int_{-\infty}^{0} < S_x^{III}(y) > dy$$

$$= \frac{K_x K_2^{y2} A_2 A_2^*}{\mu_o w K_2^{y2} + B_3^2} \int_{-\infty}^{0} e^{2B_3 y} dy$$

$$= \frac{K_x K_2^{y2}}{\mu_o w_x K_2^{y2} + B_3^2} \frac{A_2 A_2^*}{B_3} \frac{1}{} = \frac{K_x A_2^2 (n_2^2 - n_{eff}^2)}{\mu_o w B_3 (n_2^2 - n_3^2)}$$

1.3.3 Power in the surrounding medium (air)

From Equation (1.22) the expression for E_z^I is

$$E_z^I(y) = A_2 e^{B_1 h} \left[e^{iK_2^y h} + \frac{K_2^y + B_3}{K_2^y - iB_3} e^{iK_2^y h} \right] e^{-B_1 y}$$

and $\langle S_x^I \rangle = \frac{k_x}{u\ 2} E_z^I E_z^x$

$$= \frac{K_x}{2\mu_o w} A_2 A_2^* e^{2B_1 h} \left[e^{iK_2^y h} + \frac{K_2^y + iB_3}{K_2^y - iB_3} e^{iK_2^y h} \right] \left[e^{iK_2^y h} + \frac{K_2^y - iB_3}{K_2^y + iB_3} e^{iK_2^y h} \right] e^{-2B_1 y}$$

$$= \frac{2K_x A_2 A_2^*}{\mu_o \omega} e^{2B_1 h} \frac{K_2^{y2}}{(K_2^{y2} - K_1^{y2})} e^{-2B_1 y} \qquad \text{----------(1.29)}$$

The integral power flow in the air is given by

$$P^I = \int_h^\infty \langle S_x^I(y) \rangle \, dy.$$

$$= \frac{K_x A_2 A_2^*}{} e^{2B_1 h} \frac{K_2^{y2}}{(k_2^{y2} - K_1^{y2})} \int_h^\infty e^{-2B_1 y} \, dy$$

$$= \frac{K_x A^2 K_2^{y2}}{u_o w(k_2^{y2} + B_1^2)} \cdot \frac{1}{B_1} \quad \text{---------- (1.30)}$$

The total power in the substrate, film and air is obtained by adding equations (1.26) (1.28) and (1.30).

$$P\Sigma = P^I + P^{II} + P^{III}$$

$$= \frac{K_x A_2^2}{\mu_o w} \left[\frac{K_2^{y2}}{B_1 (K_2^{y2} + B_1^2)} + \frac{(m_2^2 - n_{eff}^2)}{B_3(n_2^2 - n_3^2)} + h + \frac{B_1}{K_o^2(n_2^2 - n_1^2)} + \frac{B_3}{K_o^2(n_2^2 - n_3^2)} \right]$$

$$= \frac{K_x A_2^2}{\mu_o w} \left[\frac{K_o^2 n_2^2 - K_o^2 n_{eff}^2 + B_1^2}{B_1 K_o^2 (n_2^2 - n_1^2)} + \frac{K_o^2 (n_2^2 - n_{eff}^2) + B_3^2}{B_3 K_o^2 (n_2^2 - n_3^2)} + h \right]$$

$$P\Sigma = \frac{K_x A_2^2}{\mu_o w} \left[h + \frac{1}{B_1} + \frac{1}{B_3} \right]$$

1.3.4. Normalized power flow calculations.

$$\langle S_N^I \rangle = \frac{P^I}{P\Sigma} = \frac{\frac{K_x A_2^2}{u_o w} \cdot \frac{K_o^2 (n_2^2 - n_{eff}^2)}{B_2 K_o^2 (n_2^2 - n_1^2)}}{\frac{K_x A_2^2}{} \left[h + \frac{1}{B_1} + \frac{1}{B_3} \right]}$$

$$= \frac{n_2^2 - n_{eff}^2}{B_1 (n_2^2 - n_1^2) \left[h + \frac{1}{B_1} + \frac{1}{B_3} \right]}$$

$$< S^{III} > = \frac{(n_2^2-n_{eff}^2)}{\sqrt{n_{eff}^2 - n_3^2(n_2^2-n_3^2)}\ [K_o h + \frac{1}{\sqrt{n_{eff}^2-n_1^2}} \frac{1}{\sqrt{n_{eff}^2-n_3^2}}]}$$

$$< S_N^{III} > = \frac{(n_2^2-n_{eff}^2)}{\sqrt{n_{eff}^2-n_3^2}\ (n_2^2-n_3^2)\ [2\pi \frac{h}{\lambda_o} + \frac{1}{\sqrt{n_{eff}^2-n_1^2}} + \frac{1}{\sqrt{n_{eff}^2-n_3^2}}]} \quad \text{---(1.3}$$

$$<S_N^{II}> = \frac{PII}{P\Sigma} = \frac{\left[h+B_1\frac{B_1}{K_o^2(n_2^2-K_1^2)} + \frac{3\ B_3}{K_o^2(n_2^2-n_3^2)}\right] K_x A_2^2/\mu_o w}{[h+\frac{1}{B_1}+\frac{1}{B_3}]\ \frac{K_x A_2^2}{\mu_o w}}$$

$$h+\frac{k_o(n_{eff}^2-n_1^2)^{\frac{1}{2}}}{K_o^2(n_2^2-n_1^2} + \frac{K_o(n_{eff}^2-n_3^2)^{\frac{1}{2}}}{K_o^2(n_2^2-n_3^2)} \quad \text{---- (1.33)}$$

$$h+\frac{1}{K_o(n_{eff}^2-n_1^2)^{\frac{1}{2}}} + \frac{1}{K_o(n_{eff}^2-n_3^2)^{\frac{1}{2}}}$$

The graphs for $< S_N^i >$ i = I, II, III dependent upon n_{eff} are shown at fig. 1.5.

The graphs show that total power flow is concentrated in the substrate if $n_{eff} \longrightarrow n_3$, (that is when $h \rightarrow h$ crit, at λ = const) or in the film, if $n_{eff} \rightarrow n_2$ (that is when $h \rightarrow \infty$, at λ = const.)

Fig.1.5 Normalized power flow in the layers of a single film optical waveguide with $n_1=1.0$, $n_2=1.6$, $n_3=1.5$ at $\lambda=0.6328\mu m$ vs effective refractive index n_{eff}.

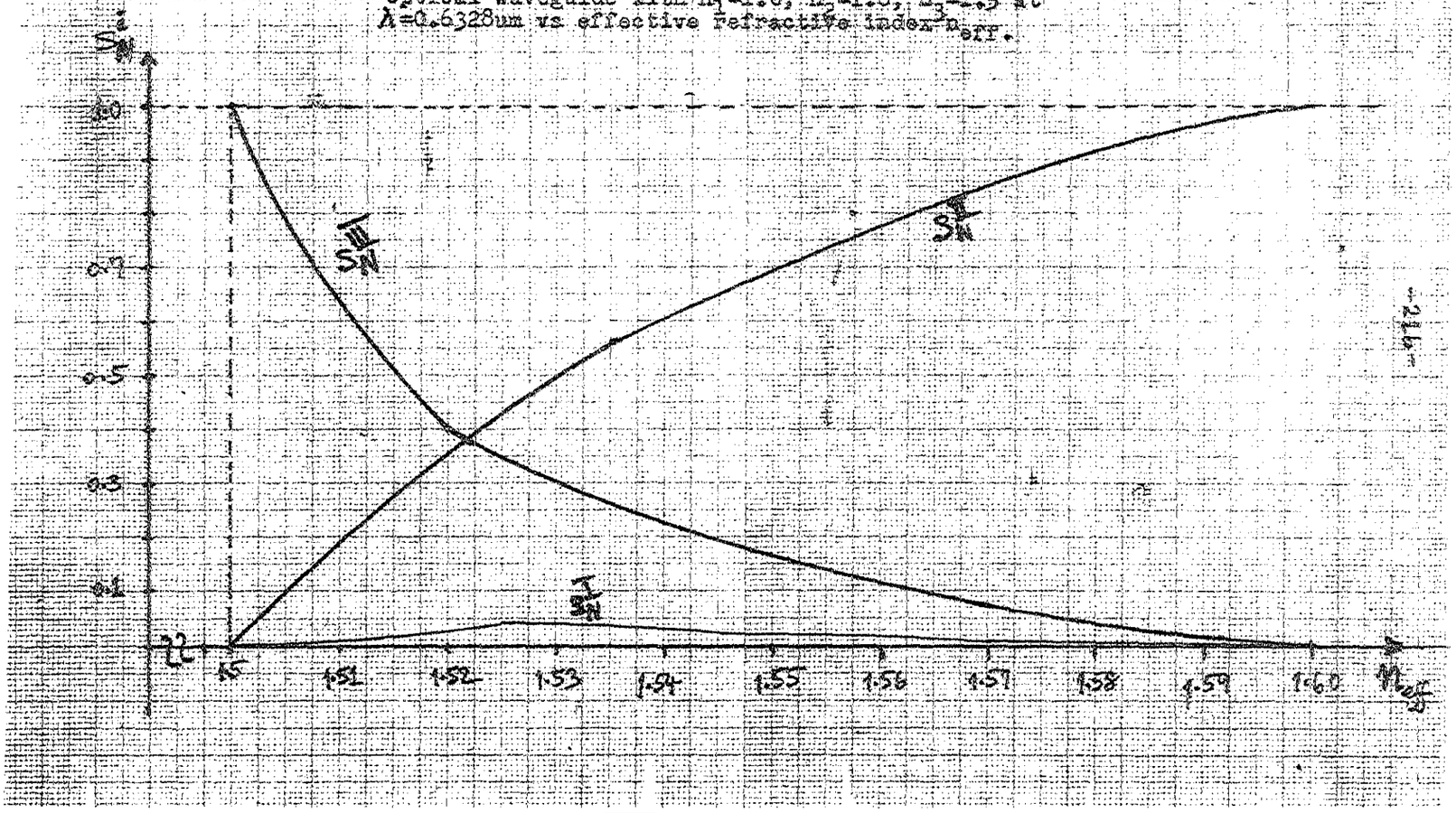

1.4 Planar analogues of bulk lenses

In general bulk lenses can be regarded as optical elements which are capable of forming converging (or diverging) spherical waves at their exit pupils. In planar optics we deal with cylindrical waves instead of spherical waves. In both cases the phase velocity changes are essential for the lenses functioning. In bulk optics the phase velocity is a function of the bulk refrative index of the medium where the light propagates.

In planar optics, as it follows from the dispersion equation (1.17) phase velocity is a function of all the bulk refractive indices of the media which constitute the optical waveguide and besides that it is a function of the film thickness.

$$U_x = f(h/\lambda , n_1(\lambda) , n_2(\lambda), n_3(\lambda))$$

It means that planar optics has got one more possibility in the realizatio of lenses, that is, by proper shaping the thickness h of the waveguiding film.

Now let us pass to the description of planar analogues of bulk lenses of various types and finally to unique planar lenses, specific only for planar optics.

1.4.1 Fresnel diffration lens

In the Fresnel diffraction lens known in bulk optics part of the diffracted light is used to produce the phenomena of focusing. This part of the light is chosen from the total difracted light according

to a special rule by means of the mask shown in figure 1.6. The shaded areas of the mask are covering that part of the light that would interfere destructively at the focal point P.

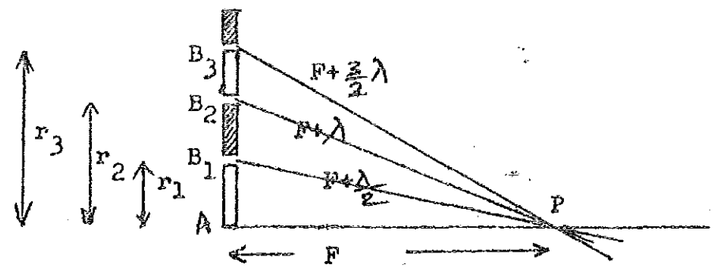

Fig.1.6 Diagram of Fresnel zones formation

This can be readily understood [9], by referring to figure 1.6 in which r_1 is shown as the radius that makes $B_1P-AP=B_1P-F=\frac{\lambda}{2}$ where F is the focal distance of the lens. Radiation reaching P from points beyond B_1 will be more than half a cycle oout of phase with th axial radiation and therefore will interfere destructively with it, thus reducing the radiaton at P. We must go to point B_2 before positive contributions are again obtained, where (B_2P-F) equals the wavelength. Therefore this part of the radiation is obstructed by a nontransparent shiled B_2B_2.

Clearly, circles with radii r_1r_2, ..., will divide the plane of the diaphragm into zones called Fresnel Zones, such that contributions within each zone will differ by no more than half a cycle in phase. The radii of the circles that form the Fresnel Zones are readily found by applying the Pythagorean theorem to the triangle APB_1 shown in figure 1.6.

This yields

$$r_n^2 + f^2 = (f + \frac{n\lambda}{2})^2 \qquad \text{----------(1.34)}$$

$r_1 = f^2+f\lambda - f^2+\frac{\lambda^2}{4} \approx \sqrt{f\lambda}$

$r_2 = f^2+\lambda^2+2f\lambda - f^2 \approx \sqrt{2f\lambda} = \sqrt{2}\sqrt{f\lambda}$

$r_3 = f^2+\frac{9}{4}\lambda^2+3f\lambda - f^2 \approx \sqrt{3f\lambda} = \sqrt{3}\sqrt{f\lambda}$

As the light waves pass through the apertures they are diffracted and focused at the focal point. Since only half of the light is diffracted in the direction to the optical axis and since only half of that part is used for focusing the efficiency of such absorbing Fresnel lens is not exceeding 25%.

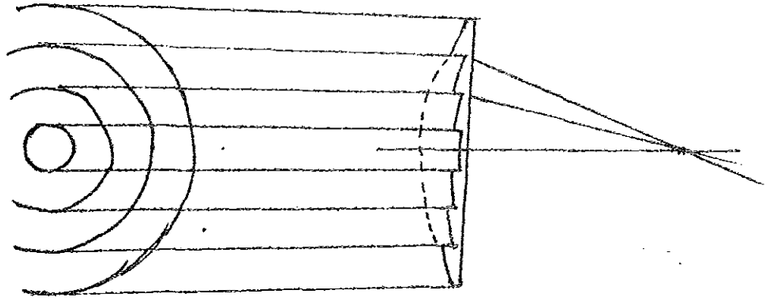

Fig. 1.7 non-absorbing phase shift Fresnel lens structure.

An alternative type of Fresnel lens is shown in figure 1.7. Lenses with spherical surfaces can become quite bulky, especially when the diameter is large and exceeds the radius of curvature; but, because refraction takes place only at the surfaces, plane parallel annular slabs can be removed from the lens without seriously imparing its function. After this removal the remaining annular segments can be telescoped to make them roughly coplanar and to yield a far lighter Fresnel lens as shown in figure 1.7.

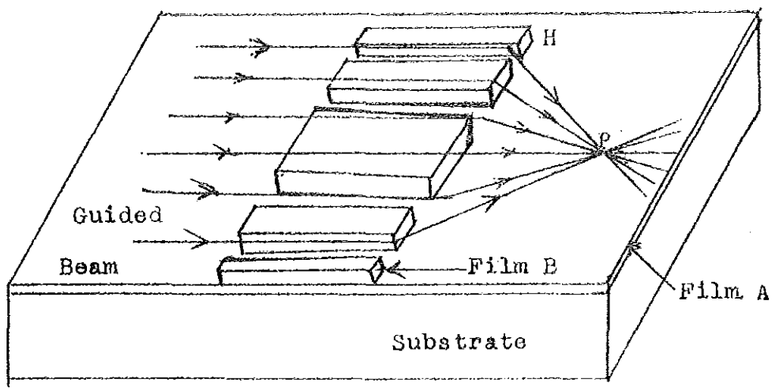

a) 3-d side view

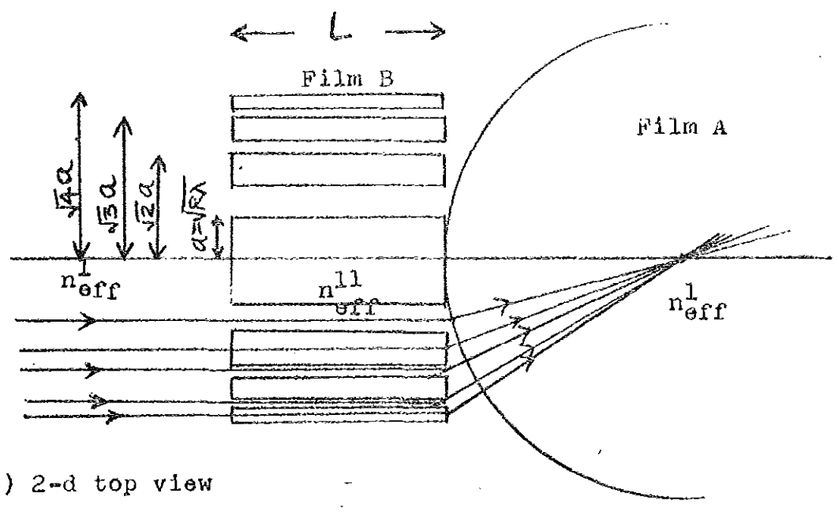

b) 2-d top view

Fig.1.8 Planar non-absorbing phase shift Fresnel lens prepared on the basis of two film optical waveguic

In this lens light from all Fresnel zones intefere constructively at the focal point P. This is achieved by introducing a phase shift equal to π in all the even Fresnel zones. Since there is no absorption the efficiency of this lens is upto 50%

Planar Fresnel Lens

The latter type of Fresnel lens is advantageous to be realized in integrated optics format. A relevant design is shown in figure 1.8. The position and transverse size of segments of additional film B displaced on the surface of the original waveguiding film A are chosen according to the specification of Fresnel zones,

$$r_i = \sqrt{f \frac{\lambda}{n_{eff}}} \times \sqrt{i}, \quad i=1,2,3, \ldots \text{----------(1.35)}$$

The longitudinal size L and the thickness H of these segments are chosen according to the dispersion equation so as to produce a phase shift equal to π for a waveguided mode.

$$k_o n_{eff}^{II}(H) \cdot L = \pi \text{ ----------(1.36)}$$

Fresnel lenses have the following drawbacks.

i) only upto 50% of the passing light can be focused

ii) the aperture of the beam to be focused cannot be large since the size of Fresnel's zones is becoming too small at the periphery of the lens and cannot be manufactured with relevant accuracy, usually

$$\Delta r = r_{i+1} - r_i = \sqrt{\frac{f\lambda}{n_{eff}^{II}}} \cdot (\sqrt{i+1} - \sqrt{i}) \geq \frac{\lambda}{2}$$

iii) The efficiency is sensitive to the variation of the ine width to space width ratio obtained in the lithographic process. [10]

Fig.1.9 Thin-film structure

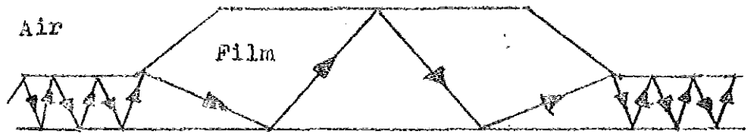

a)Cross-sectional view and zig-zag model

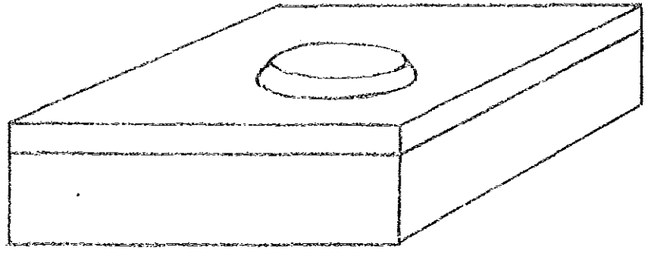

b) 3-d side view

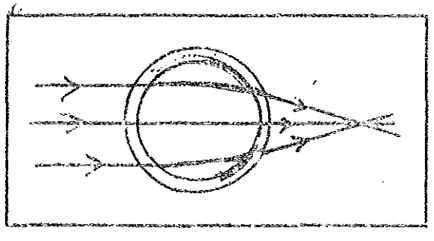

c) 2-d top view

Fig.1.9 Thin-film structure

d)Light tracks in a thin-film lens, taken from Scie ntific American Journal 1

e) Refraction in a thin-film prism, (Sc. Am. J)

1.4.2. Thin-film lens.

The phase velocity [11] of the wave's forward direction of travel in a thin-film waveguide depends besides n_j, j=1,2,3, on the thickness of the film; the velocity is higher in a thinner film and lower in a thicker film. A thinner film can be joined to a thicker one by a tapered section. If the taper is gradual enough and covers a distance of many obtical wavelenceths, a light wave can propagate from the thinner film into the thicker through the taper without being scattered.

A lens can be made in a thin-film waveguide by depositing a uniform film on the substrate and then adding another layer on top of the first through a mask with a circular opening. Since the light wave propagates more slowly through the thicker lens than through the thinner film surrounding it, it is refracted as it enters or leave the lens in precisely the same way it would be if it were going through an ordinary bulk lens. As a result the circular portion of the thin-film wave guide constitutes a thin-film lens. See fig. 1.9. The advantage of these lenses is that they are very small and simple to make; hence many of them can be formed sinulta neously in a single step to produce planar optical systems like a planar collimator, for example. Unfortunately this type of lens the same aberrations as its 3-d analogue, that is spherical aberration coma, and 1-d. astigmatism.

1.5 Unique Planar Lenses.

1.5.1. Geodesic Lens.

Consider a planar dielectric plate as an optical waveguide substrate. Prior to depositing the thin-film waveguide material, a

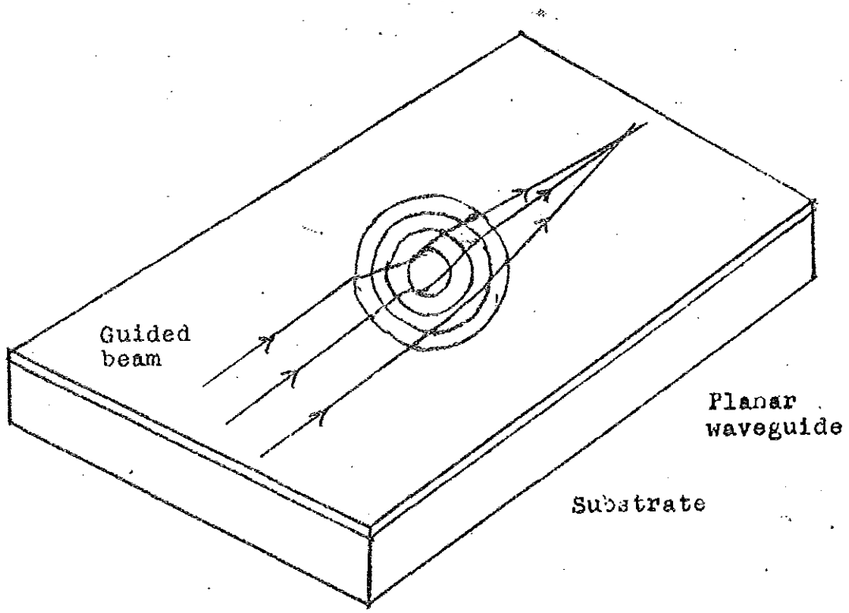

Fig.1.1B Geodesic lens 3-d side view.

shallow spherical depression is drilled into the substrate. The waveguide layer material (which has an index bigger than that of the substrate) is deposited with a uniform thickness everywhere on the substrate, including the region over the depresion. [12]

For a beam of light coupled into this optical waveguide, this depression will act like a lens and tend to focus the beam in the plane of the waveguiding film. To understand this, consider a ray in the waveguide as it encounters the depression. The waveguiding properties of the deposited layer will keep the ray from jumping over the depression (especially if the edge is slightly rounded). Thus the ray enters the depression region. Its actual path may be ascertained from a consideration of Fermat's principle (see Ch. III). It turns out that the extremum optical path is one that follows a geodesic line over the curved depression. Thus, for spherical depressions, this is along an arc of a great circle.

Now consider the projection of these paths in the plane of the waveguide. The incident rays exhibit a change in direction at the entrance (and exit) of the waveguide depression region. The behaviour of the projected rays is somewhat analogous to a ray plot of a meridional fan through a lens wherein an abrupt change in the direction of the rays occur at the lens boundaries. In bulk lenses, this bending occurs because of optical path variations from one ray to the next as a result of a refractive index change. In the case of the waveguide depression (or geodesic lens as they are called), the index may be uniform and the optical path variation results from a change of the actual

geometrical path length encountered by rays entering different parts of the depression.

The geodesic lenses have the following drawbacks.

i) If the depression is of a spherical shape, the lens has a spherical aberration.

ii) It is impossible to make geodesic lenses with small $\frac{F}{D}$ numbers, (where F is the focal distance, D is the aperture of the beam to be focused,) since it requires deep depressions of the substrate that occupy big areas on the surface of the substrate.

1.5.2 Chirp-grating lens

The scattering of the electromagnetic waves by the atoms in a lattice gives rise to a reinforced scattered wave when Bragg's condition is satisfied; that is

$$2d \sin \Theta = n\lambda$$

where d is the spacing between the planes and O is the angle that the direction of propagation makes with the lattic planes. In other words for the reflected waves to interfere constructively the change in the phase shift between them must be integer multiple of 2π. Therefore

$\Delta\Phi = \frac{2\pi}{\lambda} n \; 2d \sin O = 2\pi N$ Where N is an integer number. Hence $2d \sin \Theta = \frac{N\lambda}{n}$ ----------(1.37)

n refractive index of the medium.

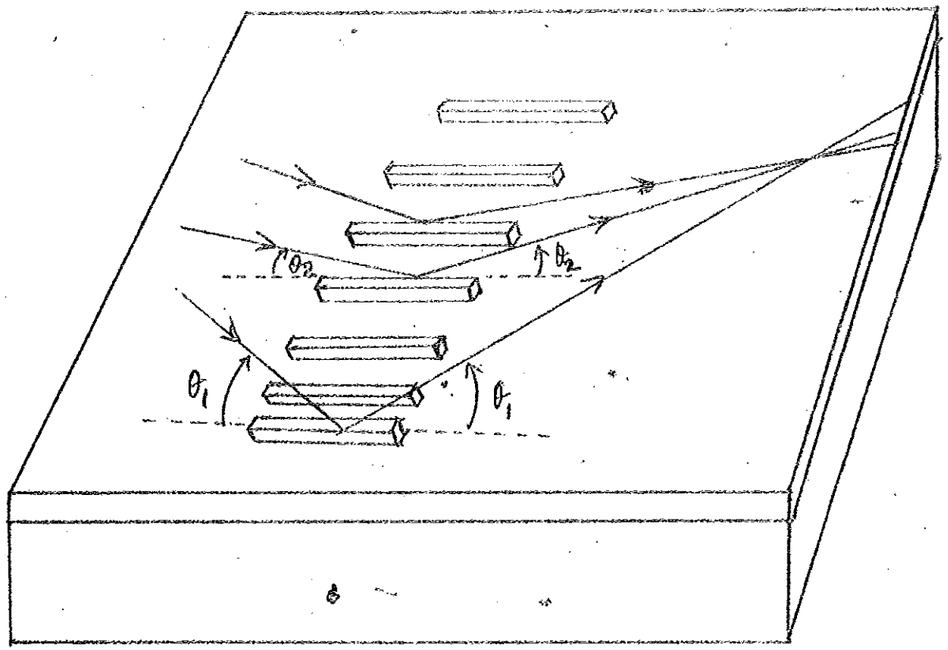

a) 3-d side view

Fig.1.11 Chirp-grating lens structure.

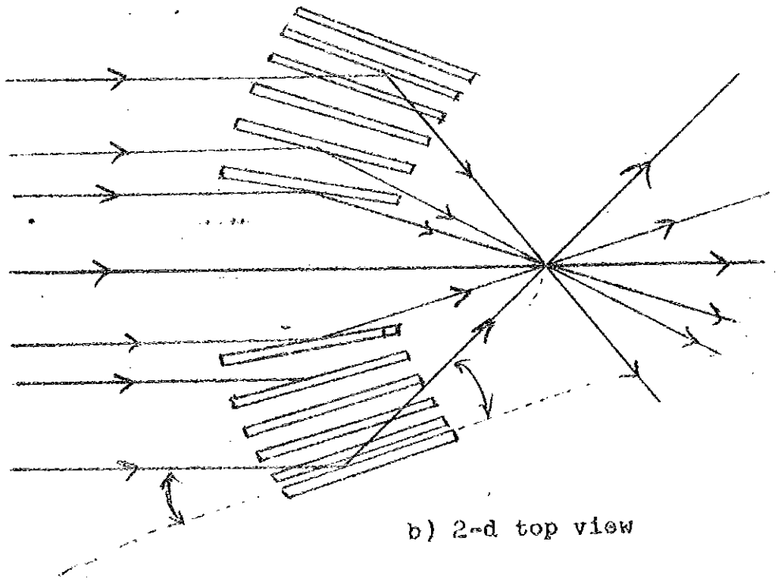

b) 2-d top view

This type of lens takes the advantage of Bragg diffraction on the phase grating prepared in the waveguide. The phase grating is made in a form of parallel strips of the same or different material put on the upper surface of the original film, thus producing regular regions with increased effective refractive index. The light entering the region of the waveguide with periodically changing effective refractive index experiences diffraction described by Bragg's law

$$2d \sin \theta = \frac{\lambda}{n_{eff}} \qquad \text{---------- (1.38)}$$

The integer N is taken equal to unity since for phase grating with sinusoidal variations of n_{eff} the contribution of the orders of diffraction higher than the first are negligibly small [senior project].

The focusing effect is achieved through simultaneously inversely changed d and θ as shown in figure 1.11, which at the same time satisfy eq. (1.35). Since the phase diffraction grating is used upto 100% of the light can be focused.

The disadvantage of this lens lies in its relatively small aperture, due to technnological difficulties in producing d less than 0.2 μm for the optical range.

1.5.3. Planar Gradient lens.

It is known [13] that for beams which propagate in a single plane (say along OX in the XOZ plane, see fig 1.12) the law for the variation in the refractive index n

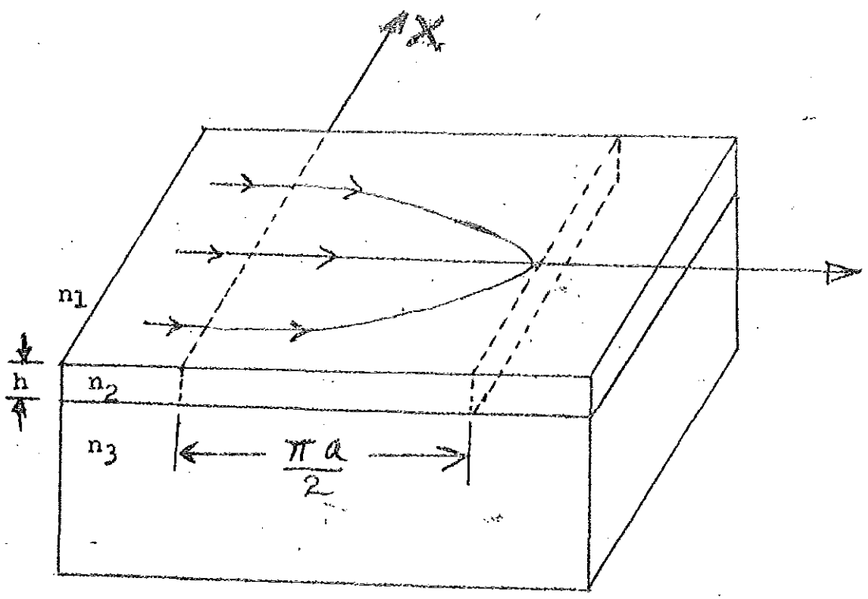

Fig.1.13 The planar gradient index lens structure.

$$n(Z) = \frac{n_o}{\cosh\left(Z/a\right)} \qquad \text{----------(1.39)}$$

where a = is a constant

n_o = is the non-gradient refractive index of the medium at of X<0. ensures focusing of a parallel beam of light at the OX axis at the distance equal to $\frac{\pi a}{2}$.

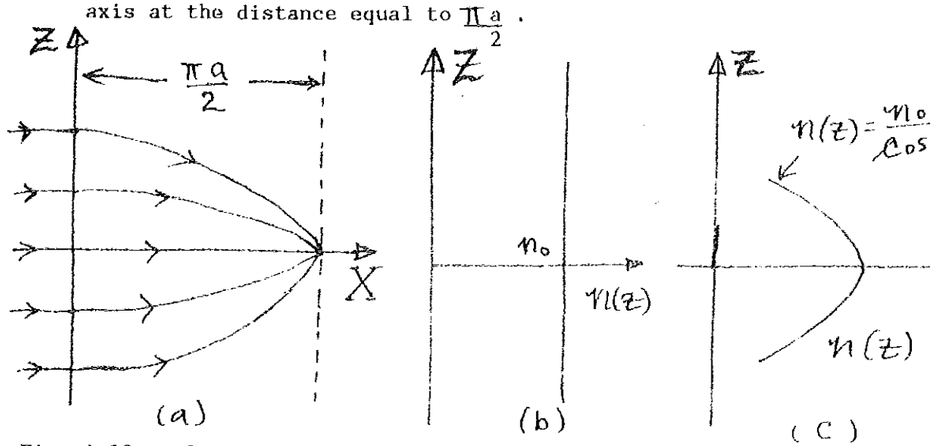

Fig. 1.12 - Focusing in gradient layered index media (a) and bulk refractive index distribution outside the lens (b) and inside the lens region (c).

Such focusing phenomena takes place in natural conditions in the atmospher and in the ocean.

The same approach is used in planar thin-film gradient lenses, where the waveguided light propagating in XOZ plane is focused as shown in fig. 1.13.

The principal difference lies only in the substitution of bulk refractive index in eq. (1.39) by its effective refractice analog (n_{eff} used in planar optics. Of course, it should be taken into

consideration that n_{eff} depends upon the bulk refractive indices n_1, $n_2 n_3$ of the materials used for the optical waveguide and the thickness h of the film, see fig. 1.13.

The required variations in n_{eff} in principle can be achieved through changes introduced in one of the bulk refractive indices n_1, n_2, or n_3. This can be done by, a gradual change in the chemical composition or structure of the material. [14] by adding diffused dopants for example by ion implanation [15].

Let's estimate the requirements for the bulk index gradients for a planar gradient index lens with

$$\frac{\pi a}{2} = 1 \text{ cm and } X_{max} = 1 \text{ cm.}$$

First we use eq.(1.39) to find the required gradient of n_{eff}.

$$\frac{\partial n_{eff}}{\partial z} = n_{eff}\,(-1)\,\frac{1}{\cosh^2\left(\frac{z}{a}\right)}\,\sinh\left(\frac{z}{a}\right)\,\frac{1}{a} \qquad \text{------(1.40)}$$

Substitution of teh above mentioned conditions gives:

$$\frac{\partial n_{eff}}{\partial z} \approx +0.574\; n_{o_{eff}}\; \text{cm.}^{-1} \approx 0.861\; 1/\text{cm}$$

Next let's treat the dispersion equation of the optical waveguide as a generalized function:

$$F\left(\frac{h}{\lambda}, n_1, n_2, n_3, n_{eff}\left(\frac{h}{\lambda}, n_1, n_2, n_3\right)\right) = 0 \qquad \text{---(1.43)}$$

Then according to the rules of differential calculus we get

$$\frac{\partial F}{\partial n_1} + \frac{\partial F}{\partial n_{eff}} \cdot \frac{\partial n_{eff}}{\partial n_1} = 0$$

$$\frac{\partial F}{\partial n_2} + \frac{\partial F}{\partial n_{eff}} \cdot \frac{\partial n_{eff}}{\partial n_2} = 0 \qquad \text{-------- (1.42)}$$

$$\frac{\partial F}{\partial n_3} + \frac{\partial F}{\partial n_{eff}} \frac{\partial n_{eff}}{\partial n_3} = 0$$

Using eq. (4) we can find the corresponding derivatives:

$$\frac{\partial n_{eff}}{\partial n_j} = - \frac{\partial F / \partial n_j}{\frac{\partial F}{\partial n_{eff}}} \quad \text{where } j = 1,2,3 \text{ -----(1.43)}$$

Direct calculation (see appendix III), brings us to the formulas.

[19]

$$\frac{\partial n_{eff}}{\partial n_1} = \frac{n_1(n_2^2 - n_{eff}^2)}{2\pi n_{eff}(n_2^2 - n_1^2)\sqrt{n_2^2 - n_1^2}\left[\frac{h}{\lambda} + \frac{1}{2\pi\sqrt{n_{eff}^2 - n_1^2}} + \frac{1}{2\pi\sqrt{n_{eff}^2 - n_3^2}}\right]}$$

$$\frac{\partial n_{eff}}{\partial n_2} = \frac{n_2}{2\pi n_{eff}}\left[2\pi\frac{h}{\lambda} + \frac{\sqrt{n_{eff}^2 - n_1^2}}{n_1^2 - n_1^2} + \frac{\sqrt{n_{eff}^2 - n_3^2}}{n_2^2 - n_3^2}\right] \cdot \frac{1}{\left[\frac{h}{\lambda} + \frac{1}{2\pi\sqrt{n_{eff}^2 - n_1^2}} + \frac{1}{2\pi\sqrt{n_{eff}^2 - n_3^2}}\right]}$$

$$\frac{\partial n_{eff}}{\partial n_3} = \frac{n_3(n_2^2 - n_{eff}^2)}{2\pi n_{eff}(n_2^2 - n_1^2)\sqrt{n_{eff}^2 - n_1^2}\left[\frac{h}{\lambda} + \frac{1}{2\pi\sqrt{n_{eff}^2 - n_1^2}} + \frac{1}{2\pi\sqrt{n_{eff}^2 - n_3^2}}\right]}$$

The graph at fig. 1.14 show how $\frac{\partial n_{eff}}{\partial n_j}$ depend upon n_{eff}. From fig. 1.2.14 it is clear that maximum values of $\frac{\partial n_{eff}}{\partial n_j}$ are of the order of 1. Therefore $(\Delta n_{eff}) \propto \Delta n_j$

From experimental data [15] it is known that Δn_{max} is of 0.29. Direct calculation through formula (1.40) indicates

that such index gradient can result in lenses with a focal distance not less than 10 cm.

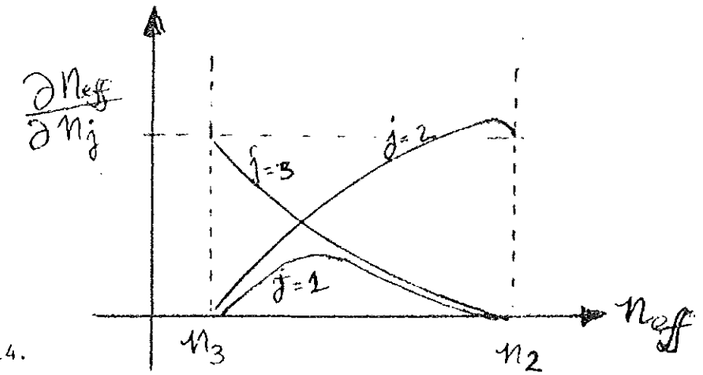

Fig. 1.14.

Dependence of n_{eff} upon changes introduced in the refractive index of the surrounding medium (j = 1) of the film (j = 2), of the substrate (j =3).

1.5.4 Generalized Luneburg Lens.

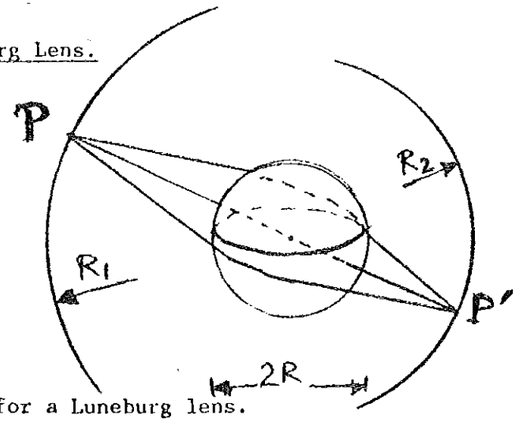

Fig. 1.15 General set up for a Luneburg lens.

Originally Luneburg lenses were designed for a microwave rang with wavelength of the order of 3 cm. and were used as scanning antennas. In general a Luneburg lens is a variable-index spherically symmetric refracting structure that will form perfect geometrical images of two given concentric spheres on each other see fig. 1.15.

One of the spheres may be of infinite radius, in which case the lens will perfectly focus a paralell beam of rays see, fig. 1.17.

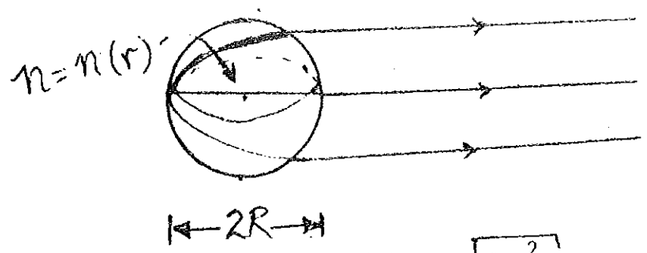

Fib. 1.16 Classical Luneburg lens $n(r) = n_o\sqrt{2-\frac{r^2}{R^2}}$ operating wit $R_1=R$, $R_2=\infty$

Luneburg [17] derived an integral equation for the summetric index profiles and solved it explicitly for the case of focusing a parallel beam to an image surface coincident with the lens, see fig. 1.1.6. Such typed of lens received a name classical Luneburg lens and its refractive index distribution is given by

$$n(r) = n_o\sqrt{2 - (r/R)^2} \qquad \text{----------(1.45)}$$

Where R- is the radius of the lens

n_o - the refractive index of the surrounding medium.

By "generalized" Luneburg lens we refer to those that give a perfect image of an infinite object at the spherical surfaces located at distances greater than one lens radius from the center of the lens, see fig. 1.17

A spherically symmetric index distribution in this case satisfies the integral equation [18]

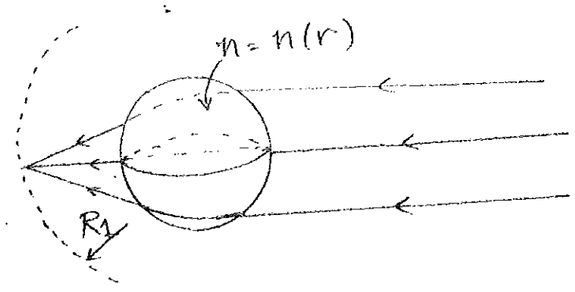

Fig. 1.17

Generalized Luneburg lens $R_1 > R, R_2 = \infty$

$$N(r) = n_o e^{w(\rho,s)} \quad \text{-------- ---------- (1.46)}$$

where $\rho = \frac{r.\ n(r)}{R\ n_o}$

and $w(p,s) = \frac{1}{\pi} \int_{\rho}^{1} \frac{\arcsin\ (x/s)}{(x^2-p^2)^{\frac{1}{2}}}\ dx$ ---------- (1.47)

and $S = \frac{f}{R}$ - $f = R_1$ focal distance measured from the center of the lens.

For the case S = 1 (classical Luneburg lens) the above integral may be evaluated in closed form. (see Appendix IV)

$$w(\rho,1) = \ln \sqrt{1+\sqrt{1-p^2}} \quad \text{----------(1.48)}$$

Therefore, substituting the result from (1.48) to formula (1.46), we obtain the classical result eq. (1.45).

For generalized Luneburg lenses (s> 1) we must deal with the integral in eq. (1.47) directly and it will be done lately in chap. 3.

It is important to underline that Luneburg lenses require the linear gradient of the refractive index of the order

$$\frac{\partial n}{\partial r} = \frac{\partial}{\partial r}\left(n_o \sqrt{2-(r/R)^2}\right) = n_o \frac{-r}{R^2\sqrt{2-\left(\frac{r}{R}\right)^2}} \qquad ----(1.49)$$

In the center of the lens, where r = 0 we get $\frac{\partial n}{\partial r} = 0$, but at the edge of the lens where r = R, we obtain the maximum required value of the gradient $\frac{\partial n}{\partial r} = -\frac{n_o}{R}$

For practical use, where R 1 cm it means that the linear gradient of refractive index must amount upto 1 cm^{-1}. Materials with such high index gradient do not exist now a days in the optical range and therefore perfect imaging properties of Luneburg lens cannot be realized in bulk optics.

On the other hand in integrated planar optics where we operate with effective index of refraction which is among other a function of thickness of the film (see eq. 1.17). Such high linear gradients can be realized.

Paraticular interest in generalized Luneburg lens with its absolutely perfect focusing properties has arisen in integrated optics for application to [19], Fourier transform signal-processing functions see fig. 1.18.

Summary

1. The dispersion equation for TE modes is derived. The critical thickness value is obtained. It is shown that waveguided modes exist for n_1, $n_3 < n_{eff} < n_2$ and that for symmetrical case $n_1 \Longrightarrow n_3$ we have $h_{crit} \Longrightarrow 0$.

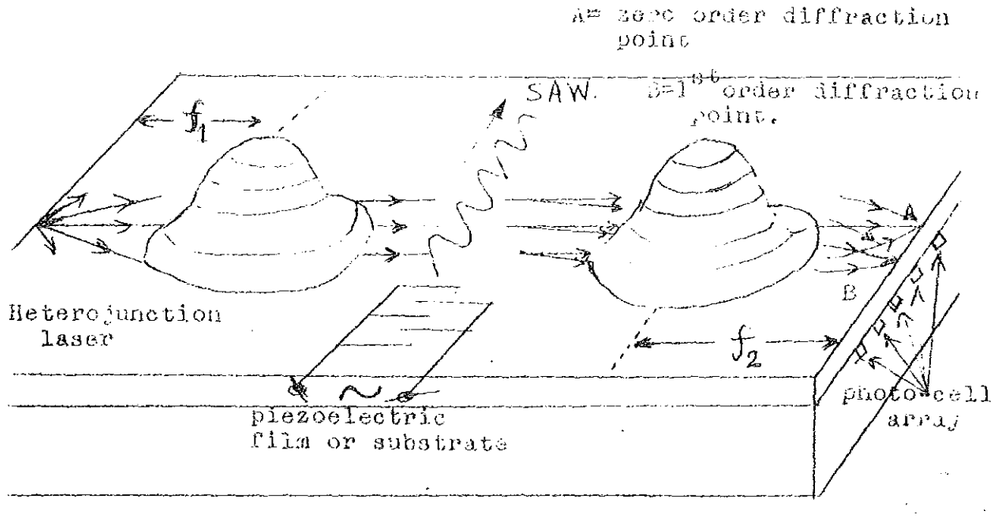

Fig.1.18 A general set-up of anintegrated optic real time spectrum analyzer.

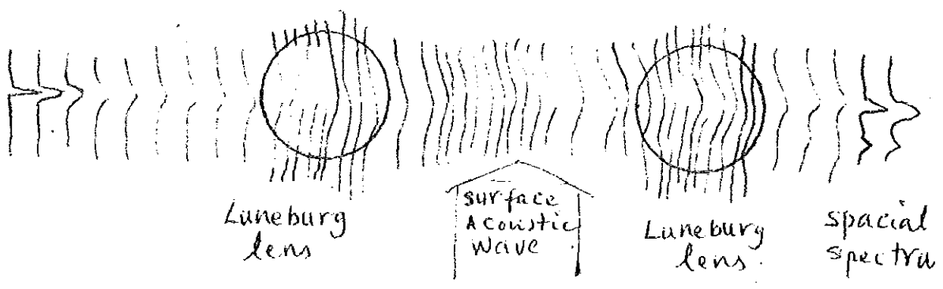

b) The evolution of the intensity ofthe propagating light inthe optical spectrum analyzer in the case,when the analyzed electrical signal contains only one harmonics.

2. Field distributions of TE modes are found. It is shown that at any value of n_{eff} part of the electric and magnetic fields penetrate beyond the boundaries of the film.

3. Power flow in the optical waveguide is assessed. It is shown that at any value of n_{eff} part of the power flow is taking place beyond the boundaries of the film.

4. All types of existing planar lenses are critically analyzed. It is shown that planar generalized Luneburg lenses are one of the most advantageous for applications in integrated optical circuits.

CHAPTER TWO

Critical analysis of the existing ray tracing method for generalized Luneburg lenses.

2.1. Gradient-index ray trace

The method described here was suggested first by L. Montagnino [15] and modified and applied to the planar Luneburg lens problem by W.H. Southwell [16]

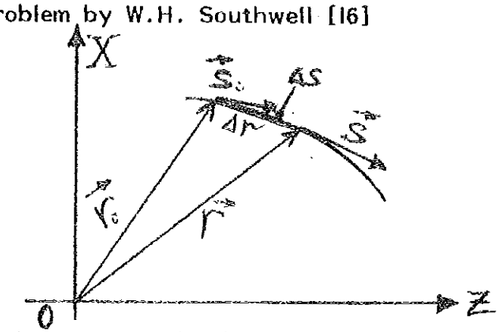

Fig. 2.1 Ray path geometry showing ray position vector $\vec{r}$ and the unit ray vector $\vec{S}$, tangent to the path.

Consider the ray path shown in fig. 2.1. The position vector $\vec{r}$ is described in a coordinate system with its origin at the center of summery "O" of the index profile.

$$\vec{r} = X\vec{i} + Z\vec{K} \quad \text{----------(2.1)}$$

The direction of the ray at a given point is given by the instanteneous tangent to the trajectory at that point and is specified by the ray vector $\vec{S}$ defined as:

$$S = \lim_{\Delta S \to 0} \frac{\Delta \vec{r}}{\Delta S} = \frac{dr}{s} = \alpha \hat{i} + \gamma \hat{K} \quad \text{----------(2.2)}$$

Where scalar ΔS is the distance along the trajectory between two neighbouring points; $\Delta \vec{r}$ is the displacement vector and α, γ - are so called the direction cosines of the ray.

Suppose we know the initial position (x_o, z_o) and direction (α_o, γ_o) at one point in space. To find the position in a close neighbourhood, we expand $\vec{r}=\vec{r}(s)$ in a Taylor's series about the known point. The argument s is the scalar distance along the ray trajectory. (2.3)

$$\vec{r}(S_o + \Delta S) = \vec{r}(S_o) + \frac{d\vec{r}}{ds}\Big| \Delta S + \frac{1}{2} \frac{d^2\vec{r}}{ds^2}\Big|_{S=S_o} (\Delta S)^2 + \cdots$$

The first derivative $\frac{d\vec{r}}{ds}$ is the ray vector $\vec{S}$ itself, The second derivative is the so-called curvature vector $\vec{K}$:

$$\vec{K} = \frac{d^2\vec{r}}{ds^2} = \frac{d}{ds}\left(\frac{d\vec{r}}{ds}\right) = \frac{d}{ds}(\vec{S}) \quad \text{-------(2.4)}$$

Thus expansion (2.3) may be written as

$$\vec{r}(s_o + \Delta S) = \vec{r}(s_o) + \vec{S}_o \cdot \Delta S + \frac{1}{2} \vec{K} \cdot (\Delta S)^2 + \ldots \text{--(2.5)}$$

Similarly we can expand the ray vector $\vec{S}$ about the same known point:

$$S(S_o + \Delta S) = \vec{S}(s_o) + \frac{d\vec{S}}{ds}\Big|_{S=S_o} \Delta S + \frac{1}{2} \frac{d^2\vec{S}}{ds^2}\Big|_{S=S_o} \cdot (\Delta S)^2 + \ldots$$

$$= \vec{S}(s_o) + \frac{d^2\vec{r}}{ds^2}\Big|_{S=S_o} \Delta S + \frac{1}{2} \frac{d}{ds}\left(\frac{d^2\vec{r}}{ds^2}\right)\Big|_{S=S_o} \cdot (\Delta S)^2 + \ldots$$

$$= \vec{S}(S_o) + \vec{K}_o \cdot \Delta S + \frac{1}{2} \frac{d\vec{K}}{ds}\Big|_{S=S_o} (\Delta S)^2 \quad \text{--------- (2.6)}$$

The required derivatives are obtained from the differential equation for the ray position in a gradient-index medium.

$$\frac{d}{ds}\left(n \cdot \frac{d\vec{r}}{ds}\right) = \vec{\nabla} n \quad \text{---------- (2.7)}$$

where $\vec{\nabla} n = \frac{\partial n}{\partial x}\hat{i} + \frac{\partial n}{\partial z}\hat{k}$ ---------- (2.8)

is the index gradient.

Expansion of eq. (2.7) gives

$$\frac{dn}{ds}\frac{dr}{ds} + n \cdot \frac{d^2\vec{r}}{ds^2} = \vec{\nabla} n$$

$$\frac{dn}{ds}\vec{S} + n\vec{K} = \vec{\nabla} n$$

$$\vec{K} = \left(\vec{\nabla} n - \frac{dn}{ds}\vec{S}\right)\frac{1}{n} \text{----------2.9)}$$

Making use of the index distribution n = n(r);

On the other hand $\vec{r} = \vec{r}(S)$

Hence $n = n(r(s))$

Therefore

$$\frac{dn}{ds} = \frac{dn}{d\vec{r}}\frac{d\vec{r}}{ds} = \frac{dn}{d\vec{r}}.\vec{S} \text{----------(2.1(}$$

Where $dn = (\vec{\nabla} n)\ (d\vec{r}) = \left(\frac{\partial n}{\partial x}\hat{i} + \frac{\partial n}{\partial z}\hat{k}\right)(dx\hat{i} + ($

$$dn = \frac{\partial n}{\partial x}dx + \frac{\partial n}{\partial z}dz$$

Hence $\frac{dn}{d\vec{r}} = \vec{\nabla} n$

and $\frac{dn}{ds} = \vec{\nabla} n.\vec{s}$ ----------(2.11)

Substituting eq. (2.11) in eq. (2.9) gives

$$\vec{K} = \frac{1}{n} [\vec{\nabla} n - (\vec{\nabla} n . \vec{S}) . \vec{S}] \quad \text{----------(2.12)}$$

Before obtaining the last required derivative $\frac{d\vec{K}}{ds}$ we rewrite eq. (2.12) making use of the symmetry in

$n=n(r)$. That is

$$\vec{\nabla} n = \frac{dn}{dr} \frac{\vec{r}}{r}$$

Hence $$\vec{K} = \frac{1}{n} [\frac{dn}{dr} \frac{\vec{r}}{r} - (\frac{dn}{dr} \frac{\vec{r}}{r} . \vec{s}) . \vec{s}]$$

$$= \frac{1}{n.r} \frac{dn}{dr} [\vec{r} - (\vec{r}.\vec{s}).\vec{s}]$$

$$= f(r) [\vec{r} - (\vec{r}.\vec{s}).\vec{s}]$$

Where $f(r) = \frac{1}{n.r} \frac{dn}{dr}$

Differentiating eq. (2.13) we have

$$\frac{d\vec{K}}{ds} = \frac{\partial f(r)}{\partial r} \frac{d\vec{r}}{ds} [\vec{r} - (\vec{r}.\vec{s}).\vec{s}] +$$

$$f(r) \left[\frac{\partial \vec{r}}{\partial r} \frac{d\vec{r}}{ds} - (\frac{\partial \vec{r}}{\partial \vec{r}} \frac{d\vec{r}}{ds} . \vec{s} + \vec{r} . \frac{d\vec{s}}{ds}) . \vec{s} - (\vec{r}.\vec{s}) \frac{d\vec{s}}{ds}\right]$$

Since $\frac{f(r)}{\partial \vec{r}} = \vec{\nabla} f(r) = \frac{df(r)}{dr} . \frac{\vec{r}}{r}$

$$\frac{d\vec{K}}{ds} = \frac{df(r)}{dr} \frac{\vec{r}.dr}{r\ ds} [\vec{t} - (\vec{t}.\vec{s}).\vec{s}] + f(r) [\vec{S} - (\vec{S}.\vec{S} + \vec{r}.\vec{K}).\vec{S} - (\vec{r}.\vec{S})\vec{K}$$

$$\frac{dk}{ds} = \frac{1}{r}\frac{df(r)}{dr}\, r.s\ [r-(r.s).s]$$

$$- f(r)\,[r.k).s + (r.s).k] + f(r)\,[s-(s.s).s] \text{----(2.14)}$$

$$+ f(r)\,[s-(s.s).s] \text{--------(2.14)}$$

The last term in eq. (2.14) obviously results in ZERO.

The ray tracing algorithm, therefore, is as follows.

1) From the known position (x_o, z_o) and direction cosines (α_o, γ_o) and given index value $n(r_o)$ and its gradient $\frac{dn}{dr}\Big/_{r=r_o}$ and the second derivative $\frac{d^2n}{dr^2}\Big/_{r=r_o}$ evaluate the curvature K using eq. (2.13) and its derivative using eq.(2.14) at this given point.

2) Select an incremental step size ΔS and evaluate the new position $r(s_o + \Delta s)$ and new direction $\vec{s}(s_o+\Delta s)$ from eq. (2.3) and (2.6)

3) Consiering our new position and direction as known, go back to step number one and repeat the sequence until the exit surface is reached.

2.2. Exit Boundary Location

It is necessary to consider the problem of precisely locating the ray position as it exits the lens region. For computational efficiency, the step size s is large compared to the required ray tracing tolerances. Thus, an interpolation is required once the ray has stepped outside the lens.

The procedure taken for locating the edge is as follows. We first define the function F,

$$F = R^2 - r^2 \qquad \text{----------(2.15)}$$

Where R is the lens radius and $r^2 = x^2 + z^2$ as determined by the ray position. By consideraing the last point inside the lens as the base point, we see that $\vec{r}$ becomes a function of the step size Δs. The function F then may be considered a function of ΔS, $F = F(\Delta S)$. The problem of locating the edge in then solved by finding the root ΔS that makes $F(\Delta S) = 0$. This may be done using Newton's method,

$$(\Delta S)_e = (\Delta S)_o - F \Big/ \frac{dF}{d(\Delta S)} \Big|_{\Delta S = S_o} \qquad \text{-------- (2.16)}$$

Since the functional dependence of F on ΔS is given through eq. (2.3), we have

$$\frac{\partial f}{\partial(\Delta s)} = -2\vec{r} \cdot \frac{d\vec{r}}{d(\Delta s)} = -2\vec{r}\cdot\vec{s} \qquad \text{---------- (2.17)}$$

Initially $(\Delta s)_o = 0$ at our base point inside the lens and the derivative in eq. (2.16) has already been evaluated. It is thus a simple matter to apply eq. (2.16) until $|F| < 10^{-8}$ or some prescribed small quantity.

We have now established the general procedure for ray tracing through the waveguide lens. But we have not, as yet, specified a value for the step size ΔS. To do this, let us return to a discussion of the convergence properties of the above ray-tracing algorithm.

2.3. Convergence and an extrapolation technique.

There are two factors to be considered when determining a value for the step size Δs. They are computing time and accuracy. It is important to know the accuracy of the ray heights as they leave the lenses. If the rays are being plotted and visual accuracy is sufficient, then the step size is easily determined. The ray trace may be repeated, each time reducing the step size a factor of 2, until no changes are visible on the plot.

However, when tracing diffraction - limited systems, it is necessary to have confidence that the ray trace will provide an exit height accurate to some fraction of a wavelength. They may require an extremely small step size (less than 1 μm. for $\lambda = 0.6328$ μm), and, consequently, long computing time. Therefore, the following extrapolation technique for achieving the desired accuracy with reasonable step sizes is suggested. [16]

For simplicity, let h = S be the step size. Consider the ray exit height y as a function of the (small) step size h, x=X(h). The problem is to estimate the value of y for the limit as h approaches zero. This suggests a Taylor's dexpansion:

$$x(h) = X(0) + \frac{dx}{dh} h + \frac{1}{2}\frac{d^2x}{dh^2} h^2 + \ldots \quad \text{----------(2.18)}$$

If h is assumed to be small enough that the first three terms of the expansion suffice, then one may pick an h, trace the ray, and determi $x(h) = X_1$. But there are three unknowns in eq. (2.18). Thus, two more ray traces are done, each time reducing h by a factor of 2, to gi x_2 and x_3. This gives the set of linear equations:

$$x_1 = a_1 + a_2 h + a_3 h^2$$

$$x_2 = a_1 + \tfrac{1}{2} a_2 h + \tfrac{1}{4} a_3 h^2 \qquad \text{----------(2.19)}$$

$$x_3 = a_1 + \tfrac{1}{4} a_2 h + \tfrac{1}{16} a_3 h^2$$

In matrix notation,

$$x = Ha \qquad \text{----------(2.20)}$$

which has a solution

$$a = H^{-1} x = \qquad \text{----------(2.21)}$$

where the matrix H is

$$H = \begin{pmatrix} 1 & h & h^2 \\ 1 & \tfrac{1}{2}h & \tfrac{1}{4} h^2 \\ 1 & \tfrac{1h}{4} & 16h^2 \end{pmatrix} \qquad \text{----------(2.22)}$$

If it is chosen that h = 0.025 μm, then

$$H^{-1} = \begin{pmatrix} \tfrac{1}{3} & -2 & \tfrac{8}{3} \\ -80 & 400 & -320 \\ 4266.7 & -12800 & 8533.3 \end{pmatrix} \qquad \text{----------(2.23)}$$

The solution for a_1, which is the desired estimate x(0), is

$$x = \tfrac{1}{3} x_1 - 2x_2 + \tfrac{8}{3} x_3 \qquad \text{----------(2.24)}$$

Equation (2.24) is the extrapolation formula. Note that it is a weighted mean of three ray-traced values and that the sum of th weights is unity. Furthermore, it turms out that these weighting factors are validity of eq. (2.24), of course depends on h being small enough such that the expansion (2.18) is valid.

2.4. Phase-front Calculation.

Hamilton's optics theory states that the exit coordinate X on the boundary of the lens region is related to the Hamilton's angle characteristic function as

$$X = -\frac{\partial T}{\partial \theta} \qquad \text{----------(2.25)}$$

Where θ is the exit angle and

$$T(\theta) = \int_{\theta_0}^{\theta} n\,ds \qquad \text{----------(2.26)}$$

see fig. 3.3.

The angular characteristic function $T(\theta)$ represents the optical path length along the ray trajectory through the system described by the Coordinate on the entrance pupil X_a, which definitely corresponds to the exit angle θ. Hence the phase shift produced by the lens region only can be written as

$$\Phi_{(\theta)} = T(\theta)\,\frac{2\pi}{\lambda_0} \qquad \text{----------(2/27)}$$

To utilize this theory it is assumed that $T(\theta)$ may be expressed as a power series*

$$T = C_1\theta^2 + C_2\theta^4 + C_3\theta^6 + \ldots \qquad \text{----------} \qquad (2.28)$$

Only even powers of θ are used since the phase front should be symmetrical with respect to the optical axis.

To determine these coefficients it is necessary to trace a number of rays and record the X_i Coordinates at the exit pupil (with exit boundary location problem included) and the exit angles θ_i

These data points are then fit in least squares fashion to the function.

$$\left.\frac{\partial T}{\partial \theta}\right|_{\theta=\theta_1} = 2C_1\theta_1 + 4C_2\theta_1^3 + 6\,C_3\theta_1^5 = -X_1$$

$$\left.\frac{\partial T}{\partial \theta}\right|_{\theta=\theta_2} = 2C_1\theta_2 + 4C_2\theta_2^3 + 6C_3\theta_2^5 = -X_2 \qquad \text{----------(2.29)}$$

$$\left.\frac{\partial T}{\partial \theta}\right|_{\theta=\theta_3} = 2C_1\theta_3 + 4C_2\theta_3^3 + 6C_3\theta_3^5 = -X_3$$

and from a system of algebraic equations with C_1, C_2 C_3 unknown.

The solution of this sytem gives the values for C_1, C_2 C_3 which are then substituted to the eq. (2.27) and then to (2.26) to produce the desired phase shift within the lens.

The phase front distribution at the exit pupil can be thus written as

$$\Phi = \Phi_a + \Phi_l + \Phi_b \qquad \text{---------- (2.30)}$$

Where Φ_a, Φ_b are phase shifts experienced by the propagating light in between the entrance pupil and lens, or the lens and the exit pupil respectively, see fig. 3.3 and eq. (3.21), eq. (3.22).

The pupil function is given by the expression

$$P = \exp.\ (i\Phi) \qquad \text{----------(2.31)}$$

Where Φ can be expressed in the exit pupil coordinates

$$X_b = R.\ [\sin\theta + (1-\cos\theta).,\ \tan(\theta + \theta_o] \qquad \text{-----(2.32)}$$

It may be shown [23] that the square of the Fourier transform of P yields the irradiance diffraction pattern in the focal plane.

Summary

1. The advantage of this method is in its mathematical simplicity and clear physical background.

2. On the other hand the method has a number of disadvantages.

   a) Computational complexity; ray tracing with diffraction - limited accuracy requires up to 10^4 number of incremental steps for determining the coordinate on the exit pupil for each trajectory.

   b) Computation of the second derivative $\frac{d^2n}{dr^2}$ is required throughout the whole procedure.

   c) It is necessary to solve additional problem for the value of the final incremental step in order not to miss the point on the boundary of the lens where the ray exits the lens region.

   d) Extrapolation technique is required to reach sufficient accuracy with incremental steps of reasonable size.

   e) The claculation of phase front distribution at the exit pupil requires the solution of algebraic system of equations practically for each new point of this distribution , since the procedure described in § 2.4 is unable to determine $\Phi = \Phi(x_b)$ with sufficient accuracy making use of only three points from the T (θ) function.

CHAPTER 3

An Alternative Method of Ray Tracing in planar Generalized Luneburg lenses.

3.1 Fermat's Principle for gradient index media with spherical symmetry.

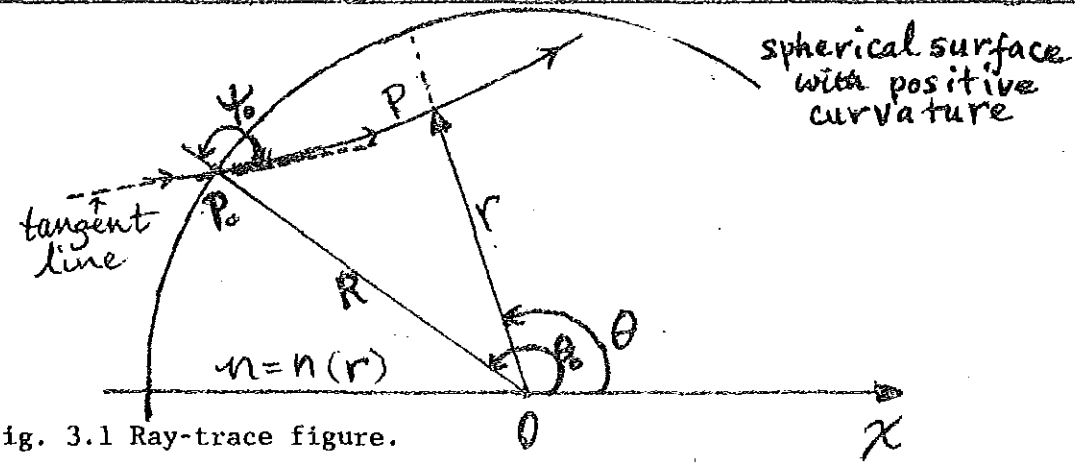

Fig. 3.1 Ray-trace figure.

Let us discuss this principle through making analysis of one particular, but practically important case: the refractive index will be assumed to have concentric summetry, that is n=n(r).

where r is the radial distance from a fixed point O. With n as a function of r, it is natural to introduce spherical coordinates (r,θ,φ) relative to "O" as origion and with the main axis along OP_o where P_o is the starting point of the ray trace, figure 3.1.

Fermat's principle states that, for a light ray joining two points P_o and P the integral

$$L = \int_{P_o}^{P} nds = \int_{P_o}^{P} n(x,yz)ds \text{ ----------(3.1)}$$

Where ds is an element of the trajectory of the ray, must be stationary relative to infinitesimal variations of the integration path joining P_o and P, see fig. 3.2.

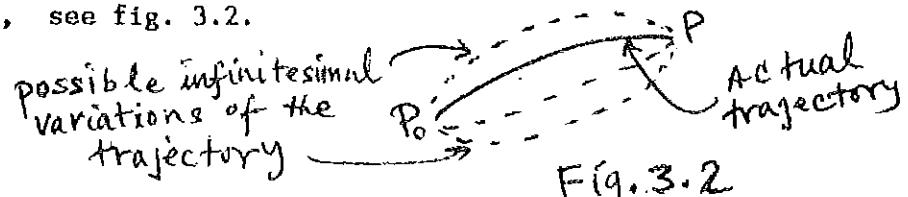

Fig. 3.2

Inother words the integral eq.(3.1) has its minimum value when the integration path exactly coincides with the actual ray trajectory.

In spherical coordinates the length of the element of the ray trajectory can be expressed as

$$dS^2 = (dr)^2 + (dr_\theta)^2 + d(r_\varphi)^2 \text{--- (3.2)}$$

where dr is the change in r with 0 and constant

and $dr_\theta = rd\theta$ ----------(5.3)

and $dr_\varphi = r\sin\theta\, d\varphi$ ---------- (3.4)

Substituting eq. (3.3) and (3.4) in eq. (3.2) gives

$$ds = (dr)^2 + r^2(d\theta)^2 + r^2 \sin^2\theta\,(d\varphi)^2$$

$$= 1+r^2\left(\frac{d\theta}{dr}\right)^2 + r^2 \sin^2\theta\left(\frac{d\varphi}{dr}\right)^2 \text{----------(3.5)}$$

Now Fermat's principle of eq. (3.1) can be expressed as

$$L = \int_R^r n(r) \quad 1+r^2\left(\frac{d\theta}{dr}\right)^2 + r^2\sin^2\theta\left(\frac{d\varphi}{dr}\right)^2 \text{----------(3.6)}$$

Where R and r denote initial and general values of the radial distance see fig. 3.1.

The problem in eq. (3.6) represents a classical one in the claculus of variations. The solution of this problem is provided by the satisfaction of the Euler equations.

$$\frac{\partial F}{\partial \varphi} = \frac{d}{dr}\frac{\partial f}{\partial \dot{\varphi}} \; ; \quad \frac{\partial f}{\partial \theta} = \frac{d}{dr}\frac{\partial f}{\partial \dot{\theta}} \text{----------(3.7)}$$

and $F(\theta, \varphi, \dot{\theta}, \dot{\varphi}, r) = n(r) \quad 1+ r^2\theta^2 + r^2\sin^2\theta\,\dot{\varphi}^2$ (3.8)

where $\dot{\theta} = \frac{d\theta}{dr}$ and $\dot{\varphi} = \frac{d\varphi}{dr}$

- 51

From eq. (3.8) we have

$$\frac{\partial f}{\partial \varphi} = \frac{\partial}{\partial \varphi}\left(n(r)\sqrt{1+r^2\dot{\theta}^2 + r^2\sin^2\theta\dot{\varphi}^2}\right) = 0 \quad \text{------(3.9)}$$

Comparison of eq. (3.9) and eq. (3.7) gives

$$\frac{d}{dr}\frac{\partial f}{\partial \dot{\varphi}} = 0 \text{ or } \frac{\partial f}{\partial \dot{\varphi}} = \text{constant.} \quad \text{----------(3.10)}$$

The result eq. (3.10) means that $\frac{\partial f}{\partial \dot{\varphi}}$ is always constant along a ray.

On the other hand, straight forward from eq (3.8), we get

$$\frac{\partial f}{\partial \dot{\varphi}} = \frac{n(r)\, r^2\sin^2\theta\dot{\varphi}}{\sqrt{1 + r^2\dot{\theta}^2 + r^2\sin^2\theta\dot{\varphi}^2}} = \text{const.} \quad \text{--- (3.11)}$$

More than that, since the choice of the OX direction is arbitrary and point P_o can be situated on the OX axis, $\theta = \pi$ and besides that it is possible that $\theta = \theta_o = \pi$ if P coincides with P_o, therefore, it is possible that $\sin\theta = 0$. It means that the constant in eq. (3.11) cann not be any other than zero.

On the other hand, since eq. (3.11) should also hold at any other value of θ, then we have to admit that it would be possible if to accept that $\dot{\varphi}$ vanish along any ray.

$$\dot{\varphi} = 0 \quad \text{----------(3.12)}$$

Equation (3.12) indicates that every ray leaving P_o is a plane curve lying in a plane containing O P_o

For nonradial ray, because of eq. (3.12), we find from eq. (3.9).

$$\frac{\partial f}{\partial \theta} = 0; \quad \frac{\partial F}{\partial \dot{\theta}} = n(r)\, r^2\dot{\theta}\,\frac{1}{\left(1+r^2\dot{\theta}^2\right)^{1/2}}$$

Hence fro m eq. 3.7.

$$\frac{d}{dr}\frac{\partial f}{\partial \dot{\theta}} = \frac{\partial f}{\partial \theta} = 0 \text{ and } \frac{\partial f}{\partial \dot{\theta}} = \text{constant} = e$$

or $$\frac{n(r)r^2\dot{\theta}}{\sqrt{1 + r^2\dot{\theta}^2}} = e \text{----------(3.13)}$$

where e is constant along the given ray with specified θ_o

As it is seen from figure 3.2.

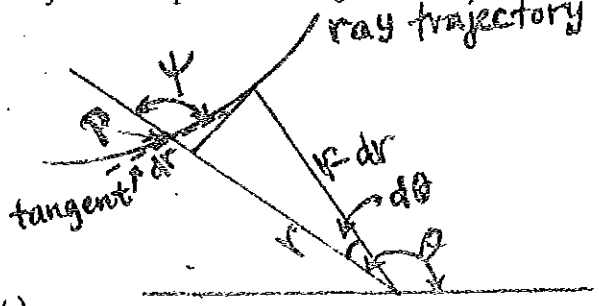

$$\tan\Psi = \tan(\pi - \Psi)$$

$$= \frac{(r-dr)d\theta}{dr}$$

$$\approx \frac{rd\theta}{dr} \propto r\dot{\theta} \text{ ---------- (3.14)}$$

fig. 3.3 ray trace figure

Ψ is the angle between the radius to the given point Pand the tangent line to the ray at this point.

Thus equation (3.13) may be written as+

$$\frac{n(r)r\tan^2\Psi}{\sqrt{1 + \tan^2\Psi}} = e$$

or $$e = \pm n(r) \cdot r\sin^2\Psi \text{ ----------(3.15)}$$

Where $\pm$ is used as $\Psi \lesseqgtr \pi/2$ respectively.

The value of e can be found from the known values at the starting point P_o. At this point eq. (3.15) becomes,

$$e = \pm n(R)R\sin\Psi_o \text{ ----------(3.16)}$$

The differential equation (3.13) can be solved in terms of a single quadrature by writing successively

$$n r^2\dot{\theta} = e\sqrt{1+r^2\dot{\theta}^2}$$

$$n^2r^4\dot{\theta}^2 \rightarrow e^2r^2\dot{\theta}^2 = e^2$$

$$r\dot{\theta}\left(n^2r^2-e^2\right)^{\frac{1}{2}} = e \cdot$$

$$r\frac{d\theta}{dr}\sqrt{n^2r^2-e^2} = e$$

$$d\theta = e\frac{1}{r\sqrt{n^2(r)^2-e^2}}\,dr$$

$$\Delta\theta = e\int_R^r \frac{1}{r}\frac{dr}{\sqrt{n^2(r)r^2-e^2}}$$

$$\theta_o - \theta = e\int_R^r \frac{1}{r}\frac{dr}{\left(n^2(r)r^2-e^2\right)^{\frac{1}{2}}}$$

$$\theta = \theta_o + e\int_r^R \frac{1}{r}\frac{dr}{\left(n^2(r)\,r^2-e^2\right)^{\frac{1}{2}}} \qquad \text{(3.17)}$$

Eq. (3.17) gives the output angle θ if the input angle θ_o, initial position R, initial inclination ψ_o and the law n(r) are specified. Explanation given by eq. (3.1) - (3.17) was taken from the Article [24]

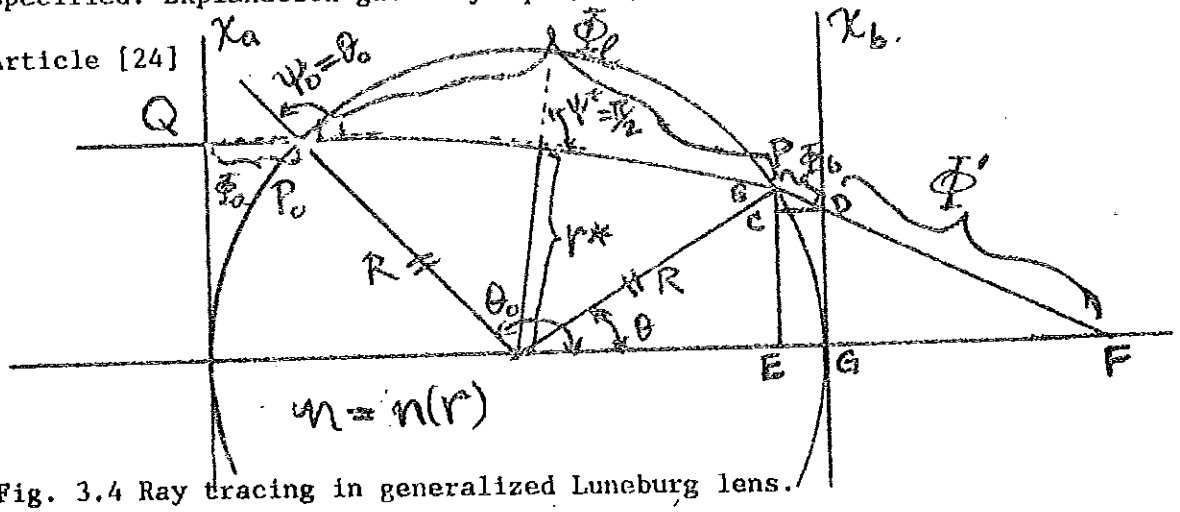

Fig. 3.4 Ray tracing in generalized Luneburg lens.

3.2. Fermat's Principle in the generalize Luneburg lenses.

Since r* is the minimum point of the trajectory and at this point the trajectory is summetric, the integral of eg. (3.17) is doubled by taking half of the ray trajectory.

That is $\theta = \theta_o + 2e\int_{r^*}^{R} \frac{1}{r}\frac{dr}{\sqrt{n^2(r)r^2-e^2}}$ ----------(3.18)

The value of r^* can be found from eq. (3.15) written as*

$$-n(R)\, R \sin\theta_o = e = -n(r^*)\, r^* \sin\psi^*$$

but $\psi^* = \pi/2$, thus

$$r^* = \frac{n(R)R \sin\theta_o}{n(r^*)} \text{ ---------- sin} \quad (3.19)$$

Note that only negative sign in eq. (3.15) has physical sense ($r^* \leq R$) for $\theta_o \geq \pi/2$.

Suppose the incident light is in a form of a parallel beam propagating along OZ, and its phase at the entrance pupil (OX_a-line) is zero everywhere, phase Φ_f at the focus F can be calculated as the sum of the phase shifts.

$$\Phi_f = \Phi_a + \Phi_\ell + \Phi_b + \Phi' \quad \text{---------(3.20)}$$

where $\Phi_\ell = \int K_o\, n(r)ds$ and ds is an element of the ray trajectory within the lens given by eq. (3.5).

From fig. (3.3)

$$\frac{CD}{\ell_b} = \cos[\pi - (\theta+\theta_o)] \Rightarrow \ell_b = \frac{CD}{\cos[\pi - (\theta+\theta_o)]}$$

But $CD = EG = R(1-\cos\theta)$

$$\ell_b = -\frac{R(1-\cos\theta)}{\cos(\theta+\theta_o)}$$ ----------

$$\therefore \quad \Phi_b = K_o\, n_H\, \ell_b = K_o n_H \frac{(-R(1-\cos\theta))}{\cos(\theta+\theta_o)} \text{ ----------(3/21)}$$

$$\Phi_a = K_o n_H R(1+\cos\theta_o) \text{ ----------(3.22)}$$

$$\Phi_\ell = \int k_o\, n(r)\, ds = 2k_o \int_{r^*}^{R} n(r)\, ds$$

$$ds = \sqrt{1 + r^2 \left(\frac{d\theta}{dr}\right)^2 + r^2 \sin^2\theta \left(\frac{d\varphi}{dr}\right)}\; dr$$

but from some steps back in eq. (3.17)

$$\frac{d\theta}{dr} = \frac{e}{r\sqrt{n^2(r)\, r^2 - e^2}}$$

$$S\theta,\ ds = \sqrt{\frac{1 + r^2 e^2}{r^2 n_{eff}^2(r) r^2 - e^2}}\; dr$$

$$dS = \frac{n_{eff}\, dr}{\sqrt{n_{eff}^2(r) r^2 - e^2}}$$

Hence $$\Phi_\ell = 2K_o \int_{r^*}^{R} \frac{n_{eff}^2(r) r dr}{\sqrt{n_{eff}^2(r) r^2 - e^2}} \qquad \text{----------(3.23)}$$

$$\Phi' = K_o\, n_H DF = K_o n_H \frac{DG}{\sin\left[\pi - (\theta + \theta_o)\right]}$$

$$\Phi' = \frac{K_o n_H DG}{\sin(\theta + \theta_o)} = \frac{K_o n_H X_b}{\sin(\theta + \theta_o)}$$

$$\Phi' = \frac{K_o n_H R[\sin\theta + (1 - \cos\theta)\tan(\theta + \theta_o)]}{\sin(\theta + \theta_o)} \qquad \text{--------(3.24)}$$

Where $X_b = DG = BE - BC = -R\sin\theta - CD\tan\left[\pi - (\theta + \theta_o)\right]$

$$= R\sin\theta + R(1 - \cos\theta)\tan(\theta + \theta_o)$$

The focal length $f = \dfrac{X_b}{\tan[\pi - (\theta+\theta_o)]}$

$$= \frac{R[\sin\theta + (1-\cos\theta)\tan(\theta+\theta_o)]}{-\tan(\theta+\theta_o)}$$

If the lens is perfect f will be independent of θ.

i.e. f = Constant.

Finally adding eq. (3.21) ---------(3.24)

$$\Phi_f = k_o n_H \frac{-R(1-\cos\theta)}{\cos(\theta+\theta_o)} + K_o n_H R(1+\cos\theta_o) + \frac{K_o n_H R[\sin\theta + (1-\cos\theta)\tan(\theta+\theta_o)]}{\sin(\theta+\theta_o)} + 2K_o \int_{r^*}^{R} \frac{n_{eff}^2(r)\,r\,dr}{\sqrt{n_{eff}^2(r)r^2-e^2}} \quad \text{---------- (3.25)}$$

For a perfect lens Φ_f is a constant value independent of θ_o

3.3. Removal of Singularity point in the exit angle integral.

The integrnd in eq. (3.18) has a singularity point at the lower limit of integration when $r = r^*$. In order to remove the singularity, let us do the following. First the integral is resolved into two:

$$\int_{r^*}^{R} \frac{1}{r}\frac{dr}{n^2(r)\,r^2-e^2} = \int_{r^*}^{r^*+\delta} \frac{dr}{r\sqrt{n(r)r-e}\sqrt{n(r)r+e}} + \int_{r^*+\delta}^{R} \frac{dr}{r\left(n^2r^2-e^2\right)^{1/2}}$$

Where δ is a small value (3.26)

Now the singularity point is contained only by the first integral which we will denote as I.

Second, let us resolve the function n(r)r into Taylor series around the point $r = r^*$

$$n(r)r \approx n(r^*)r^* + (r-r^*)\left[\frac{dn(r)}{dr}\Big|_{r=r^*} \cdot r^* + n(r^*)\right]$$

$$= e + (r-r^*)\,A \qquad \text{----------(3.27)}$$

Where $A = \left.\frac{dn(r)}{dr}\right|_{r=r^*} \cdot r^* + n(r^*)$

Hence the integral I in eq. (3.26) can be written as:

$$I = \int_{r^*}^{r^*+\delta} \frac{dr}{r\sqrt{n(r)r-e}\,\sqrt{n(r)r+e}} \approx \int_{r^*}^{r^*+\delta} \frac{dr}{r\sqrt{n(r)r-e}\,\sqrt{(r-r^*)A}} \qquad \text{----(3.28)}$$

Third, let us perform an integration by parts taking

$$du = \frac{dr}{r\sqrt{(r-r^*)}}, \qquad U = \int_{r^*}^{r^*+\delta} \frac{dr}{r\sqrt{(r-r)^*}}$$

$$= \frac{2}{\sqrt{r^*}} \arctan\sqrt{\frac{r-r^*}{r^*}}\Big|_{r^*}^{r^*+\delta} = \frac{2}{\sqrt{r^*}} \arctan\sqrt{\frac{\delta}{r^*}}$$

$$V = \frac{1}{\sqrt{n(r)r-e}}\Big|_{r^*}^{r^*+} = \frac{1}{\sqrt{n(r^*+\delta)\,(r^*+\delta)-e}} - \frac{1}{\sqrt{n(r^*)r^*-e}}$$

$$= \frac{1}{\sqrt{n(r^*+\delta)\cdot(r^*+\delta)+R\sin\theta_o}} - \frac{1}{\sqrt{2R\sin\theta_o}}$$

$$dV = -\tfrac{1}{2} \frac{}{[n(r)r-e]^{3/2}} \left(\frac{dn(r)}{dr} r + n(r)dr\right)$$

Hence from eq. (3.28) we get

$$I = \int_{r^*}^{r^*+\delta} \frac{dr}{r\sqrt{n(r)r-e}\sqrt{(r-r^*)A}}$$

$$= \frac{1}{\sqrt{A}}\left[\frac{2}{\sqrt{r^*}} \arctan\sqrt{\frac{\delta}{r^*}} \left(\frac{1}{\sqrt{n(r^*+\delta)\,(r^*+\delta)-e}}\right) + \right.$$

$$\left. + \frac{1}{\sqrt{r^*}}\int_{r^*}^{r^*+\delta} \arctan\sqrt{\frac{(r-r^*)}{r^*}} \left(\frac{\frac{dn(r)}{dr}\,r + n(r)dr}{(n(r)r-e)^{3/2}}\right)\right]$$

Substitution of the formula (3.29) into eq. (3.26) and finally into eq. (3.18) gives the following solution

$$0=\theta_0+2e\left[\frac{1}{\sqrt{A}\sqrt{r^*}}\left\{2\arctan\sqrt{\frac{\delta}{r^*}}\left(\frac{1}{\sqrt{n(r^*+\delta)\,(r^*+\delta)-e}}\right)\right.\right.$$

$$\left.\left. + \int_{r^*}^{r^*+\delta} \arctan\sqrt{\frac{(r-r^*)}{r^*}} \left(\frac{\frac{dn(r)}{dr}\,r + n(r)dr}{(n(r)r-e)^{3/2}}\right)\right\} + \int_{r^*+\delta}^{R} \frac{dr}{r\left(n^2(r)r^2-e^2\right)^{1/2}}\right]$$

--------(3.30)

Formula (3.30) looks more complicated than eq. (3.18), however, the integrand in eq. (3.30) is well behaved and the integrals can be easily evaluated by numerical methods.

In general only numerical methods are applied to this problem, since the function n(r) measured in expriment can be specified only in a form of a table.

Another more simple though less accurate form of computing the integral I in eq. (3.26) can be suggested. This approach is based on the expansion in Taylor's series of the function $n^2(r)\,r^2$.

$$n^2(r)r^2 \approx n^2(r^*)r^{*2} + \left(2n(r)\frac{dn(r)}{dr}\,r^2 + n^2(r)2r\right)\Big|_{r=r^*}^{r-r^*}$$

$$\approx n^2(r^*)r^{*2}+C(r-r^*) \quad \text{----------(3.31)}$$

Where $C = 2n(r^*)\left.\frac{dn(r)}{dr}\right|_{r=r^*} \cdot r^{*2}+n^2(r^*)2r^*$

$$= -2e\left(\left.\frac{dn(r)}{dr}\right|_{r=r^*} \cdot r^*+n(r^*)\right) = -2eA$$

now instead of eq. (3.28) we get

$$I=\int_{r^*}^{r^*+\delta} \frac{dr}{r\sqrt{n^2(r)r^2-e^2}} \approx \int_{r^*}^{r^*+\delta} \frac{dr}{r\sqrt{cr-cr^*}}$$

$$= \frac{2}{\sqrt{cr^*}} \arctan \left.\frac{\sqrt{c(r-r^*)}}{\sqrt{cr^*}}\right|_{r=r^*}^{r^*+\delta}$$

$$= \frac{2}{\sqrt{cr^*}} \arctan \frac{\sqrt{\delta}}{\sqrt{r^*}} \quad \text{----------(3.32)}$$

Hence eq. (3.18) can be written as:

$$\theta=\theta_o + 2e\left[\frac{2}{\sqrt{cr^*}} \arctan \frac{\sqrt{\delta}}{\sqrt{r^*}} + \int_{r^*+\delta}^{R} \frac{dr}{r\sqrt{n^2(r)r^2-e^2}}\right] \quad \text{----------(3.33)}$$

Let us check the accuracy of formula (3.33) for the case of a classical Luneburg lens with refractive index distribution.

$$n(r) = \sqrt{2-\frac{r^2}{R^2}} \quad , \; n(R)= 1$$

In this case we get:

$$r^* = R\sqrt{1+\cos\theta_o}$$

$$\frac{dn}{dr} = -\frac{\sqrt{1+\cos\theta_o}}{R\sqrt{1-\cos\theta_o}}$$

$$A = \frac{-2\cos\theta_o}{\sqrt{1-\cos\theta_o}} \; ; \quad c = \frac{-2R\sin 2\theta_o}{\sqrt{1-\cos\theta_o}}$$

$$A = \frac{-2\cos\theta_o}{\sqrt{1-\cos\theta_o}} \quad ; \quad C = \frac{-2R\sin 2\theta_o}{\sqrt{1-\cos\theta_o}}$$

Suppose $\delta = \xi R$, where ξ is small number, then eq. (3.33) we get.

$$2eI = \frac{-2\sqrt{\sin\theta_o}}{\sqrt{-\cos\theta_o}} \cdot \frac{\sqrt[4]{1-\cos\theta_o}}{\sqrt[4]{1+\cos\theta_o}}$$

The second integral in eq. (3.33) can be written in this case as

$$2e\int_{r^*+\delta}^{R} \frac{dr}{r\sqrt{\left(\frac{1}{R^2}\right)r^4 + 2r^2 - e^2}} = \arcsin(\cos\theta_o) \qquad \text{----(3.34)}$$

$$= \arcsin \frac{2\xi + \cos\theta_o\sqrt{1+\cos\theta_o}}{2\xi\cos\theta_o + \cos\theta_o\sqrt{1+\cos\theta_o}}$$

Finally eq. (3.33) for classical Luneberg lens can be written as:

$$\theta = \theta_o - \frac{4\sin\theta_o\sqrt[4]{1-\cos\theta_o}}{\sqrt{-2\sin 2\theta_o}\cdot\sqrt[4]{1+\cos\theta_o}} \arctan\frac{\sqrt{\xi}}{\sqrt[4]{1+\cos\theta_o}} + \arcsin(\cos\theta_o) -$$

$$- \arcsin\frac{2\xi + \cos\theta_o\sqrt{1+\cos\theta_o}}{2\xi\cos\theta_o + \cos\theta_o\sqrt[4]{1+\cos\theta_o}} \qquad \text{----------(3.35)}$$

The results of calculations according to eq. (3.35) for $\xi = 10^{-4}, 10^{-5}, 10^{-6}$ are represnted in a graph in figure 3.5.

From the graph it can be concluded

1. The exit angle error grows for $\theta \Longrightarrow \pi$, and $\theta \Longrightarrow \pi/2$.
2. By appropriate choice of ξ the accuracy can be put within diffraction - limited performance.
3. Typical value of ξ is around 10^{-5}

3.4. Removal of Singularity point in the phase front integral.

Phase shift produced by the lens is given by eq. (3.23) which contains a singularity point at $r = r^*$. Therefore, let us divide the integration range into two subranges.

$$I = \int_{r^*}^{r^*+} \frac{n^2(r)r\,dr}{\sqrt{n^2(r)r^2-e^2}} + \int_{r^*+\delta}^{R} \frac{n^2(r)r\,dr}{\sqrt{n^2(r)r^2-e^2}}$$

$$I = I_1 + I_2 \quad \text{----------(3.36)}$$

Where δ is a small number $\delta = \frac{1}{2}R$, where $\frac{1}{2}$ is again small, and $e = R\sin\theta_o = R.\cos\kappa_o$ and $\kappa_o = \theta_o - \eta_2$. Now the singularity is contained in I_1. Let us make use of eq. (3.27) in I_1. It gives:

$$I_1 = \int_{r^*}^{r^*+\delta} \frac{n^2(r)r\,dr}{\sqrt{n^2(r)r^2-e^2}} = \int_{r^*}^{r^*+\delta} \frac{n^2(r)r\,dr}{\sqrt{n(r)r-e}\sqrt{n(r)r+e}}$$

$$\approx \frac{1}{\sqrt{A}} \int_{r^*}^{r^*+\delta} \frac{n^2(r)r\,dr}{\sqrt{n(r)r-e}\sqrt{r-r^*}} \quad \text{----------(3.37)}$$

Where $A = \left.\frac{dn(r)}{dr}\right|_{r=r^*} . r^* + n(r^*)$ ----------(3.38)

Integrating by parts, where

$$du = \frac{rdr}{r-r^*}, \quad u = \int \frac{rdr}{r-r^*}$$

$$u = \frac{2}{3}(r+2r^*)\sqrt{r-r^*}$$

$$dv = \frac{\sqrt{n(r)r-e}\,(2n(r)\frac{dn}{dr}r + n(r)) - \frac{dn}{dr}r + n(r)}{2\sqrt{n(r)r-e}}\, n^2(r)dr$$

$$2\left(n(r)r-e\right)^{3/2}$$

$$= \frac{3n^2(r)r\frac{dn}{dr} + 4n^2(r)\frac{dn}{dr} - n^3(r)\,dr}{2\left(n(r)r-e\right)^{3/2}} \quad \text{----------(3.39)}$$

$$V = \frac{n^2(r)}{n(r)r-e} \quad \text{-----(3.40)}$$

Finally I_1 can be written as:

$$I_1 \approx \frac{1}{\sqrt{A}} \int_{r^*}^{r^*+\delta} \frac{n^2(r)r\,dr}{\sqrt{n(r)r-e}\,\sqrt{r-r^*}} =$$

$$= [(n(r^*+\delta))^2 - n^2(r^*)]2r^*\sqrt{\delta} \leftarrow$$

$$nr^*+\quad)(r^*+\quad -3 \qquad -2e$$

$$= r^*\sqrt{\delta} \int_{r^*}^{r^*+\delta} \frac{3n^2(r)\left[\frac{dn}{dr}\right]-en(r)\frac{dn}{dr}-n^3(r)dr}{(n(r)r-e)^{3/2}} \qquad \text{---------(3.41)}$$

Although eq. (e.4) appears more complicated, it is actually "well behaved" and may be easily evaluated numerically.

Let us derive less complicated though also less accurate expression for I_1. Substitution of eq. (3.31) in I_1 gives:

$$I_1 = \int_{r^*}^{r^*+\delta} \frac{n^2(r)r^2\,dr}{r\sqrt{n^2(r)r^2-e^2}} = \int_{r^*}^{r^*+\delta} \frac{e^2+c(r-r^*)\,dr}{r\sqrt{c(r-r^*)}}$$

$$= \frac{e^2}{\sqrt{c}} \int_{r^*}^{r^*+\delta} \frac{dr}{r\sqrt{r-r^*}} + \sqrt{c} \int_{r^*}^{r^*+\delta} \frac{\sqrt{r-r^*}}{r}\,dr$$

$$= \frac{e^2}{\sqrt{c}} \int_{r^*}^{r^*+\delta} \frac{dr}{r\sqrt{r-r^*}} + \sqrt{c} \left(2\sqrt{r-r^*}\,\Big|_{r^*}^{r^*+\delta} - r^* \int_{r^*}^{r^*+\delta} \frac{dr}{r\sqrt{r-r^*}} \right)$$

$$= \left(\frac{e^2}{\sqrt{c}} - r^*\sqrt{c}\right) \frac{2}{\sqrt{r^*}} \arctan \frac{\sqrt{r-r^*}}{\sqrt{r^*}}\Bigg|_{r^*}^{r^*+\delta} + 2\sqrt{c}\sqrt{\delta}$$

$$I_1 = \frac{2(e^2 - \sqrt{c}r^*)}{\sqrt{cr^*}} \arctan \frac{\sqrt{\delta}}{\sqrt{r^*}} + 2\sqrt{c\delta} \qquad \text{----------(3.42)}$$

Once again from eq. (3.41)

$$c = 2\left(n(r^*)r^*r^*\frac{dn}{dr}\Big|_{r=r^*} + n(r^*)r^* \cdot n(r^*)\right)$$

$$= 2e\left(r^*\frac{dn}{dr}\Big|_{r=r^*} + n(r^*)\right) \text{ ----------(3.43)}$$

Let us check up the accuracy of eq. (3.42) and thus the accuracy of the basic formula eq. (3.37) using classical Luneburg lens with refractive index distribution.

$$n(r) = n_0\sqrt{2-\frac{r^2}{R^2}}, \quad \frac{dn}{dr} = \frac{1}{n(r)}\left(\frac{-r}{R^2}\right)$$

In this case

$$r^* = R\sqrt{1-\sin\alpha_0}\ ;\ n(r^*) = \sqrt{1+\sin\alpha_0}$$

$$C = 4R\sin\alpha_0\sqrt{1-\sin\alpha_0}$$

$$\frac{e^2}{\sqrt{cr^*}} - \sqrt{cr^*} = \frac{R(1-4\sin\alpha_0 + 3\sin^2\alpha_0}{2\sqrt{\sin\alpha_0\,(1-\sin\alpha_0)}}$$

Finally eq. (3.42) may be written as:

$$I_1 \simeq \frac{R(1-4\sin\alpha_0 + 3\sin^{-2}\alpha_0)}{\sqrt{\sin\alpha_0\,(1-\sin\alpha_0)}}\arctan\sqrt{\frac{2}{\sqrt[4]{1-\sin\alpha_0}}} +$$

$$+ 4R\sqrt{2}\sqrt{\sin\alpha_0}\sqrt[4]{1-\sin\alpha_0} \text{ ----------(3.44)}$$

Now let us pass to the calculation of the integral I_2 in eq.(3.40)

$$I_2 = \int_{r^*+\delta}^{R} \frac{n^2(r) r\,dr}{\sqrt{n^2(r)r^2 - e^2}} = \int_{r^*+\delta}^{R} \frac{(2 - r^2/R^2) r\,dr}{\sqrt{(2 - \frac{r^2}{R^2})\, r^2 - e^2}} \qquad \text{---------(3.45)}$$

Introducing new variable $t = r^2$, $r = \sqrt{t}$, $r^3 = t\sqrt{t}$, $dr = \frac{dt}{2\sqrt{t}}$

the integral in eq. (3.44) can be written as:

$$I_2 \quad 2 \int_{(r^*+\delta)^2}^{R^2} \frac{\sqrt{t}\,dt}{2\sqrt{t}\sqrt{(-\frac{1}{R^2})t^2 + 2t - e^2}} - \frac{1}{R^2} \int_{(r^*+\delta)^2}^{R^2} \frac{t\sqrt{t}\,dt}{2\sqrt{t}\sqrt{(-\frac{1}{R^2})t^2 + 2t - e^2}}$$

$$= \int_{(r^*+\delta)^2}^{R^2} \frac{dt}{\sqrt{X}} - \frac{1}{2R^2} \int_{(r^*+\delta)^2}^{R^2} \frac{t\,dt}{\sqrt{X}}$$

Where $X = (-\frac{1}{R^2})\, t^2 + 2t - e^2$

$$I_2 = \frac{1}{2} \left(\sqrt{X} \Big|_{(r^*+\delta)^2}^{R^2} + \int_{(r^*+\delta)^2}^{R^2} \frac{dt}{\sqrt{X}} \right)$$

But $(r^*+\delta)^2 \simeq r^{*2} + 2r^*\delta = R^2(1 - \sin\alpha_0) + 2R^2\varepsilon\sqrt{1 - \sin\alpha_0}$

After a number of sinmplifications,

$$I_2 = \frac{R}{2} \left(\sin\alpha_0 - 2\sqrt{\varepsilon}\,\sqrt{\sin\alpha_0}\,\sqrt[4]{1 - \sin\alpha_0} + \arcsin\left(\frac{1 - 2\varepsilon\sqrt{1 - \sin\alpha_0}}{\sin\alpha_0}\right) \right)$$

--------(3.46)

Substituting eq. (3.46) and eq. (3.44) into eq. (3.40) and then into eq. (3.37) gives:

$$\Phi_{\ell} = k_o R \left[\frac{2\left(1-4\sin\alpha_o + 3\sin^2\alpha_o\right)}{\sqrt{\sin\alpha_o\left(1-\sin\alpha_o\right)}} \arctan \frac{\sqrt{\varepsilon}}{\sqrt[4]{1-\sin\alpha_o}} + \sin\alpha_o + \right.$$

$$\left. + 6\sqrt{\varepsilon}\sqrt{\sin\alpha_o}\ \sqrt[4]{1-\sin\alpha_o} + \arcsin\left(1-\frac{2\varepsilon\sqrt{1-\sin\alpha_o}}{\sin\alpha_o}\right)\right]$$

The test value for Φ_{ℓ} at $\alpha_o = \pi/2$ can be calculated straight forward.

$$\Phi_{\ell}(\alpha_o = \pi/2) = 2K_o\varepsilon\int_o^R \left(2-r^2/R^2\right)dr = k_o R\left(1+\frac{\pi}{2}\right) \quad \text{------(3.48)}$$

The same result as in eq. (3.48) should also follow from eq. (3.47) and eq. (3.36) at any arbitrary value of α_o according to the following.

$$\Phi = \Phi_{\ell}(\alpha_o) + \Phi_a(\alpha_o) = \Phi_{\ell}(\alpha = \pi/2), \quad \text{-----3.49)}$$

Comparison of results calculated through eq. (3.48) and eq. (3.49) can be seen from figure 3.6.

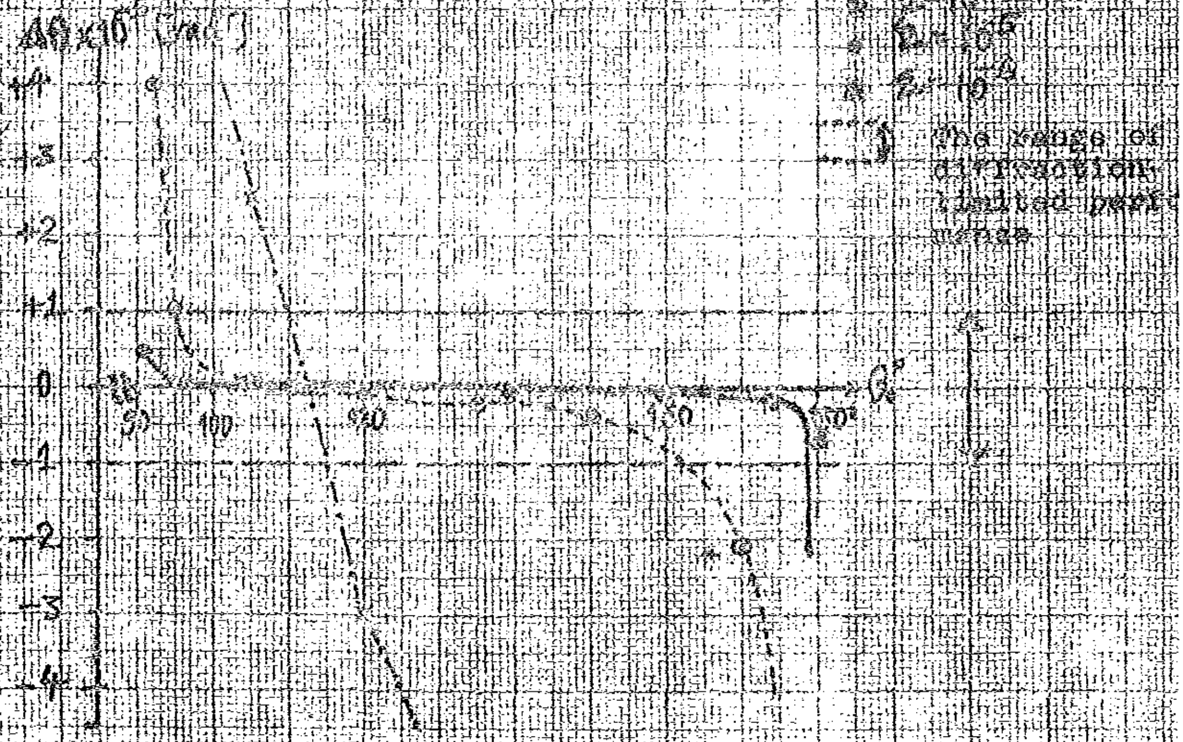

Fig.3.5 The out put angle error ψ as a function of the input angle θ_0 for classical Luneburg lens taken at different proportions of the integrals I_1 and I_2 in eq.

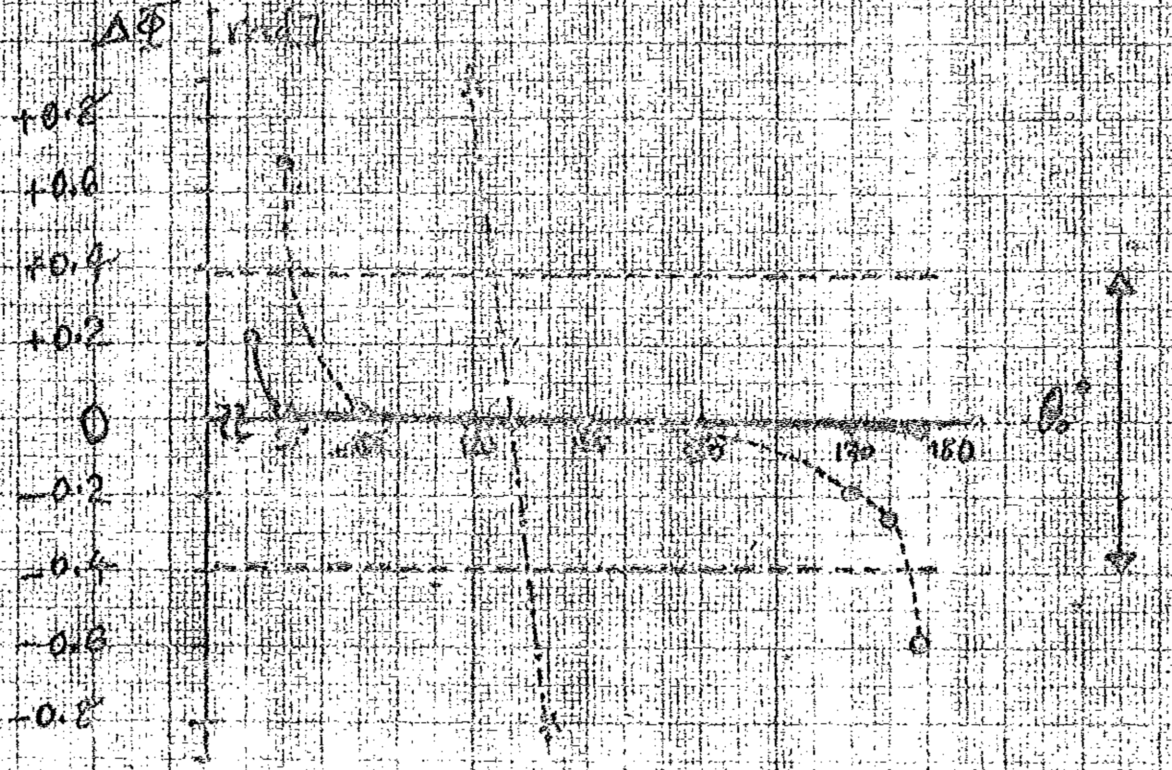

Fig.3.6 The phase error at the exit pupil of the classical Luneburg lens as a function of the input angle θ_0

The Out-put angle error as a function of the input angle θ_o for classical Luneburg lens taken at different proprotions of the integrals I_1 and I_2 in eq.(3.35)

When $\xi = 10^{-4}$

θ_o	θ	$\Delta\theta$ (rad)
91° = 1.5882496 rad	1.583705394	r0.2 x 10^{-5}
95° =1.658062789 rad	1.658052126	1.066 x10^{-5}
105° =1.832595714 rad	1.832595014	0.07 x 10^{-5}
120° =2.094395102 rad	2.094396072	-0.097 x 10^{-5}
135° =2.35619449 rad	2.35619672	-0.2082 x 10^{-5}
150° =2.617993878	2.617997957	-0.408 x 10^{-5}
170° =2.967059728	2.967081114	-2.14 x 10^{-5}
175° =3.054326191	3.054387488	-6.13 x 10^{-5}
179° =3.124139361	3.124817353	-67.8 x 10^{-5}

When $\xi = 10^{-5}$.

θ_o	θ(rad)	$\Delta\theta$(rad)
91°	1.588245233	0.44 x 10^{-5}
95°	1.658062508	0.028 x 10^{-5}
175°	3.054328136	-0.1945 x 10^{-5}
179°	3.I24161104	-2.17 x 10^{-5}

when $\xi = .10^{-6}$

179°	3.124140065	-7.043 x 10^{-7}

When $\varepsilon = 10^{-3}$

θ_o	θ_o (rad)	θ (rad)	$\Delta\theta$ (rad)
91°	1.588249619	1.583868349	454.42×10^{5}
105°	1.832595714	1.832570451	2.5×10^{-5}
120°	2.094395102	2.094425622	-3.05×10^{-5}
135°	2.35619449	2.356259491	-6.5×10^{-5}
150°	2.617993878	2.618124149	-13.02×10^{-5}
170°	2.967059728	2.96773509	-66.53×10^{-5}
175°	3.054326191	3.056215021	$-188.881. \times 10^{-5}$
179°	3.124139361	3.143090922	-1895.15×10^{-5}

as a function of the input angle θ_0.

exact = 127629.5015 rad.

$\varepsilon = 10^{-4}$

θ_0	$\Phi = \Phi_a + \Phi_\ell$ (rad)	$\Delta\Phi$ (rad)
91°	127622.1614	7.34
95°	127628.8158	0.6857
105°	127629.3854	0.1161
120°	127629.4737	0.0278
135°	127629.5504	-0.0489
150°	127629.5907	-0.0892
170°	127629.6864	-0.1849
175°	127629.7651	-0.2631
179°	127630.0944	-0.5929

$\varepsilon = 10^{-5}$

θ_0	$\Phi = \Phi_a + \Phi_\ell$	$\Delta\Phi$ (rad)
91	127629.2698	0.2317
95°	127629.4798	0.0217
105°	127629.4978	0.0037
120	127629.5015	0.0000
135	127629.5031	-0.0016
150	127629.5043	-0.0028
170	127629.5075	-0.0060
175	127629.5096	-0.0081
179	127629.5204	-0.0189

$\varepsilon = 10^{-3}$

θ_0	$\Phi = \Phi_a + \Phi_\ell$	$\Delta\Phi$
120°	127628.6208	0.8807
135°	127631.046	-1.54
305	127625.8266	+3.67

From the graph it can be concluded:

1. The phase front error grows as $\theta_0 \Rightarrow \pi$ and $\theta_0 \Rightarrow \pi/2$
2. By appropriate choice of ℓ the accuracy can be put within diffraction - limited performance.
3. Typical value of is about 10^{-5}

3.5. An experimental sample of Luneburg lens.

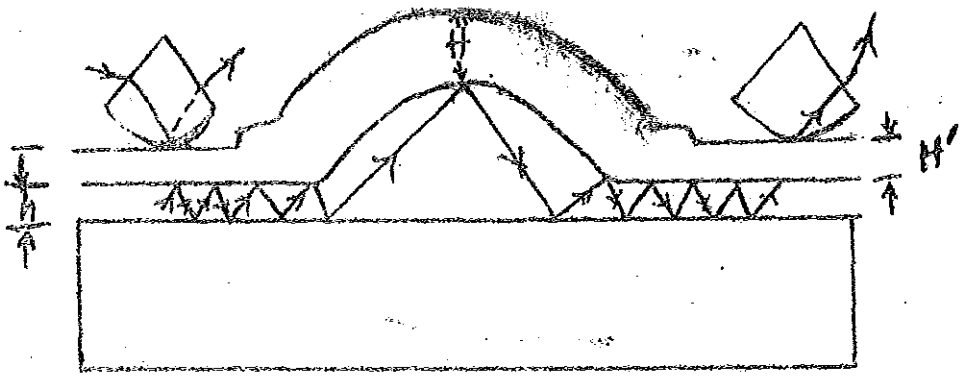

Fig. 3.7. General side view of Luneburg lens made of Ta_2O_5 film (n=2.15) deposited on the glass substrate (n=1.51) and covered by additional protective PMMA (organic glass) film (n=1.49) which is tapered to smaller thickness H' 0.9 μm under the coupling and the decoupling prisms.

The structure and materials of the examined Luneburg lens and the whole set up is shown in figure 3.7. Ta_2O_5 film used in the sample was obtained by cathode sputtering. The Luneburg lens region of the film was prepared by additional cathode sputtering of Ta_2O_5 material through an aluminium mask of a conical shape. The protective coating of organic glass film was deposited by drawing from the solution.

Figures 3.8 - 3.11 describe light tracks of TE_0 mode at λ = 0.6328 um in the described waveguide optical system. On all four photos the entrance pupil of the lens is on the left side.

Fig. 3.8-3.10 show how a narrow beam propagates through Luneburg lens region. Observe the smooth change of the direction of propagation at fig. 3.8 and 3.9 typical only for gradient effective index lenses. A bright point on the extreme right corresponds to the reflection of the ray shown at fig. 3.- on the left side wall of the decoupling prisom. Its position indicates the transverse X_a coordinate at the beam at the entrance pupil of the Luneburg lens. Note that the lens region looks like concentric coloured circles being exposed to external non-monochromatic radiation.

Fig. 3.11 was prepared in the absence of external non-monochromatic radiation, while a narrow beam was displaced to several discrete positions along the entrance pupil of the lens to demonstrate focusing phenomena. The focal length of the lens measured from the center is 12.1 mm, lens aperture 11.6 mm, a relative aperture 1:1.043.

A smaple of the Luneburg lens studied in this thesis was prepared in radiophysics laboratory of the Peoples' Friendship University, Moscow [25].

Fig.3.8

Fig.3.9

Fig.3.10

Fig.3.11

Summary

1. Fermat's principle for a generalized Luneburg case is formulated. An equation for a minimum current radius value is derived. Singularity points in the integrands for the exit angle and the phase shift in the lens region are obtained.

2. Two possible ways of the removal of the singularity points in the integrands are suggested. It is shown that the desired diffraction - limited performance is achieved by a proper choice of a small parameter ξ introduced in the method. Typical value of ξ is 10^{-5}, 10^{-6}.

3. An experimental sample of a planar generalized Luneburg lens is qualitatively tested. Photos of various light tracks in the lens are attached.

C O N C L U S I O N

The study carried out in this thesis supports the concept of integrated optics. It is shown that a single film optical waveguide constitutes a basic element for an integrated optical circuit.

Thanks to the dependence of effective refractive index upon the thickness of the film, unique types of lenses (like generalized Luneburg lens, geodesic lens, chirp-grating lens) can be realized in integrated optics format. Particularly the Luneburg lenses are famous for their capability of absolutely perfect imaging. These lenses are the key components of the planar optical spectral analyzers.

However, fabrication tolerances may introduce deviation from perfect performance in Luneburg lenses. Tolerances may be expected in indices of refraction of the substrate and of the film and particularly in the shape of the thickness profile of the film in the Luneburg lens region.

Ray-tracing method in such lenses developed in Chapter III of this theis may help in this case to:

a) estimate permissible fabrication tolerances which still do not violate diffraction - limited performance.

b) Predict the expected focal spot size of the Luneburg lens fabricated with given tolerances.

c) Estimate possible character and value of tolerances if the distribution of light in the focal plance is specified.

The method is based on Fermat's principle. Unfortunately the integrands contain singularity points which, however, can be overcome successfully. The resulting formulas are approximate, but the desired accuracy can be easily reached by a proper choice of the value of a small parameter ξ.

Appendix I

Derivation of eq. (1.12)

$$A_2 + B_2 - A_3 = 0$$

$$K_2^y A_2 - K_2^y B_2 + K_3^y A_3$$

$$K_2^y e^{iK^y h} A_2 - K_2^y e^{-iK_2^{yh}} B_2 - K_1^y A_1 = 0$$

$$e^{iK_2^y} A_2 + e^{-iK_2^y h} B_2 - A_{1=0}$$

Taking the determinant of the above homogeneous equation and equating it to zero give the eigen value equation.

$$\begin{vmatrix} 0 & 1 & 1 & -1 \\ 0 & K_2^y & -k_2^y & k_3^y \\ -K_1^y & K_2^y e^{iK^y h}{}_2 & -K_2^y e^{-ik^y h}{}_2 & 0 \\ -1 & e^{iK_2^y h} & e^{iK_2^y h} & 0 \end{vmatrix} = 0$$

$$= -1 \begin{vmatrix} 0 & -K_2^y & K_3^y \\ -K_1^y & -K_2^y e^{-iK_2^y h} & 0 \\ -1 & e^{-iK_2^y h} & 0 \end{vmatrix} + 1 \begin{vmatrix} 0 & K_2^y & K_3^y \\ -K_1^y & K_2^y e^{iK_2^y h} & 0 \\ -1 & e^{iK_2^y h} & 0 \end{vmatrix} + 1 \begin{vmatrix} 0 & K_2^y & -K_2^y \\ -K_1^y & K_2^y e^{iK^y h} & -K_2^y e^{-iK^y h} \\ -1 & e^{iK_2^y h} & e^{-iK_2^y h} \end{vmatrix} = 0$$

$$= -1[k_3^y(-K_1^y - K_2^y)e^{-iK_2^y h}] + 1 \; [k_3^y(-K_1^y + K_2^y)e^{iK_2^y h}] +$$

$$+ 1 \left\{ [-K_2^y(-K_1^y - K_2^y)e^{-iK_2^y h}] - K_2^y (-K_1^y + K_2^y)e^{iK_2^y h}] \right\} = 0$$

$$= (K_3^y + K_2^y)(K_1^y + K_2^y) e^{-iK_2^y h} + (K_3^y - K_2^y)(K_2^y - K_1^y)e^{iK_2^y h} = 0$$

$$\Rightarrow \frac{(K_1^y + K_2^y)}{(K_2^y - K^y)} e^{-2iK_2^y h} = \frac{(K_2^y - K_3^y)}{(K_2^y + K_3^y)}$$

Appendix II

$$F = \frac{2\pi h}{\lambda}\sqrt{n_2^2 - n_{eff}^2} - \arctan\sqrt{\frac{n_{eff}^2 - n_1^2}{n_2^2 - n_{eff}^2}} - \arctan\sqrt{\frac{n_{eff}^2 - n_3^2}{n_2^2 - n_{eff}^2}} - m\pi = 0 .$$

$$\frac{\partial F}{\partial n_1} = -\frac{1}{1+\frac{n_{eff}^2 - n_1^2}{n_2^2 - n_{eff}^2}} \left[\frac{1}{\sqrt{n_2^2 - n_{eff}^2}} \cdot -2n_1 \times \frac{1}{2} \cdot \frac{1}{\sqrt{n_{eff}^2 - n_1^2}}\right]$$

$$= \frac{(n_2^2 - n_{eff}^2)\cdot n_1}{(n_2^2 - n_1^2)\sqrt{n_2^2 - n_{eff}^2}\sqrt{n_{eff}^2 - n_1^2}} = \frac{n_1\sqrt{n_2^2 - n_{eff}^2}}{(n_2^2 - n_1^2)\left(\sqrt{n_{eff}^2 - n_1^2}\right)}$$

$$\frac{\partial F}{\partial n_3} = -\frac{1}{1+\frac{n_{eff}^2 - n_3^2}{n_2^2 - n_{eff}^2}} \cdot \frac{1}{\sqrt{n_2^2 - n_{eff}^2}} \cdot \frac{1}{2} \cdot \frac{2n_3}{\sqrt{n_{3ff}^2 - n_3^2}}$$

$$= \frac{n_3\sqrt{n_2^2 - n_{eff}^2}}{(n_2^2 - n_3^2)\sqrt{n_{eff}^2 - n_3^2}}$$

$$\frac{\partial F}{\partial n_2} = \frac{2\pi h}{\lambda}\frac{(+n_2}{\sqrt{n_2^2 - n_{eff}^2}} + \frac{1}{\frac{1+n_{eff}^2 - n_1^2}{n_2^2 - n_{eff}^2}} \left[\frac{\sqrt{n_{eff}^2 - n_1^2}\cdot\frac{1}{2}\cdot 2n_2}{\sqrt{n_2^2 - n_{eff}^2}}\right]$$

$$+ \frac{1}{\frac{1+n_{eff}^2 - n_3^2}{n_2^2 - n_{eff}^2}} \left[\frac{\sqrt{n_{eff}^2 - n_3^2}\cdot 2n_2\cdot\frac{1}{2}}{\sqrt{n_2^2 - n_{eff}^2}}\right]$$

$$\frac{\partial F}{\partial n_2} = \frac{2\pi h}{\lambda} \frac{n_2}{\sqrt{n_2^2 - n_{eff}^2}} - \frac{n_2 \sqrt{n_2^2 - n_{eff}^2}\ \sqrt{n_{eff}^2 - n_1^2}}{(n_2^2 - n_1^2)} -$$

$$- \frac{n_2 \sqrt{n_2^2 n_{eff}^2}\ \sqrt{n_{eff}^2 - n_3^2}}{(n_2^2 - n_3^2)}$$

$$\frac{\partial F}{\partial n_{eff}} = - \frac{2\pi h}{\lambda} \frac{n_{eff}}{\sqrt{n_2^2 - n_{eff}^2}} - \frac{1}{1 + \frac{n_{eff}^2 - n_1^2}{n_2^2 - n_{eff}^2}} \left[\right.$$

$$\left. \frac{\sqrt{n_2^2 - n_{eff}^2}\ \frac{n_{eff}}{\sqrt{n_{eff}^2 - n_1^2}} - (-n_{eff}) \frac{\sqrt{n_{eff}^2 - n_1^2}}{\sqrt{n_2^2 - n_{eff}^2}}}{n_2^2 - n_{eff}^2} \right] -$$

$$- \frac{1}{1 + \frac{n_{eff}^2 - n_3^2}{n_2^2 - n_{eff}^2}} \left[\frac{(n_2^2 - n_{eff}^2)^{1/2} \frac{n_{eff}}{\sqrt{n_{eff}^2 - n_3^2}} - \frac{(-n_{eff})(n_{eff}^2 - n_3^2)^{1/2}}{\sqrt{n_2^2 - n_{eff}^2}}}{(n_2^2 - n_{eff}^2)} \right]$$

$$= \frac{2\pi h}{\lambda} \frac{n_{eff}}{\sqrt{n_2^2 - n_{eff}^2}} - \frac{n_{eff}\,(n_2^2 - n_1^2)}{(n_2^2 - n_1^2)\sqrt{n_{eff}^2 - n_1^2}\sqrt{n_2^2 - n_{eff}^2}} -$$

$$- \frac{n_{eff}\,(n_2^2 - n_3^2)}{(n_2^2 - n_3^2)\sqrt{n_{eff}^2 - n_3^2}\sqrt{n_2^2 - n_{eff}^2}}$$

$$\frac{\partial F}{\partial n_{eff}} = - \frac{n_{eff} \cdot 2\pi}{\sqrt{n_2^2 - n_{eff}^2}} \left[\frac{h}{\lambda} + \frac{1}{2\pi\sqrt{n_{eff}^2 - n_1^2}} + \frac{1}{2\pi\sqrt{n_{eff}^2 - n_1^2}} \right]$$

$$\frac{\partial n_{eff}}{\partial n_1} = -\frac{\partial F}{\partial n_1} \Big/ \frac{\partial F}{\partial n_{eff}} = \frac{n_1\sqrt{n_2^2-n_{eff}^2} \Big/ (n_2^2-n_1^2)\sqrt{n_{eff}^2-n_1^2}}{\frac{n_{eff}\,2\pi}{\sqrt{n_2^2-n_{eff}^2}}\left[\frac{h}{\lambda} + \frac{1}{2\pi\sqrt{n_{eff}^2-n_1^2}} + \frac{1}{2\pi\sqrt{n_{eff}^2-n_3^2}}\right]}$$

$$= \frac{n_1\,(n_2^2-n_{eff}^2)}{n_{eff}\,2\pi\,(n_2^2-n_1^2)\sqrt{n_{eff}^2-n_1^2}} \cdot \frac{1}{\left[\frac{h}{\lambda} + \frac{1}{2\pi\sqrt{n_{eff}^2-n_1^2}} + \frac{1}{2\pi\sqrt{n_{eff}^2-n_3^2}}\right]}$$

$$\frac{\partial n_{eff}}{\partial n_3} = -\frac{\frac{\partial F}{\partial n_3}}{\frac{\partial F}{\partial n_{eff}}} = \frac{n_3\sqrt{n_2^2-n_{eff}^2} \Big/ (n_2^2-n_3^2)\sqrt{n_{eff}^2-n_3^2}}{\frac{2\pi\,n_{eff}}{\sqrt{n_2^2-n_{eff}^2}}\left[\frac{h}{\lambda} + \frac{1}{2\pi\sqrt{n_{eff}^2-n_1^2}} + \frac{1}{2\pi\sqrt{n_{eff}^2-n_3^2}}\right]}$$

$$= \frac{n_3\,(n_2^2-n_{eff}^2)}{2\pi\,n_{eff}\,(n_2^2-n_3^2)\sqrt{n_{eff}^2-n_3^2}} \cdot \frac{1}{\left[\frac{h}{\lambda} + \frac{1}{2\pi\sqrt{n_{eff}^2-n_1^2}} + \frac{1}{2\pi\sqrt{n_{eff}^2-n_3^2}}\right]}$$

$$\frac{\partial n_{eff}}{\partial n_2} = -\frac{\frac{\partial F}{\partial n_2}}{\frac{\partial F}{\partial n_{eff}}} = \frac{\frac{2\pi h}{\lambda}\cdot\frac{n_2}{\sqrt{n_2^2-n_{eff}^2}} + \frac{n_2\sqrt{n_2^2-n_{eff}^2}\sqrt{n_{eff}^2-n_1^2}}{(n_2^2-n_1^2)} + \frac{n_2\sqrt{n_2^2-n_{eff}^2}\sqrt{n_{eff}^2-n_3^2}}{(n_2^2-n_3^2)}}{\frac{2\pi\,n_{eff}}{\sqrt{n_2^2-n_{eff}^2}}\left[\frac{h}{\lambda} + \frac{1}{2\pi\sqrt{n_{eff}^2-n_1^2}} + \frac{1}{2\pi\sqrt{n_{eff}^2-n_3^2}}\right]}$$

$$= \frac{n_2}{2\pi n_{eff}\left[\frac{2\pi h}{\lambda} + \frac{\sqrt{n_{eff}^2-n_1^2}}{(n_2^2-n_1^2)} + \frac{\sqrt{n_{eff}^2-n_3^2}}{(n_2^2-n_3^2)}\right]} \cdot \frac{1}{\left[\frac{h}{\lambda} + \frac{1}{2\pi\sqrt{n_{eff}^2-n_1^2}} + \frac{1}{2\pi\sqrt{n_{eff}^2-n_3^2}}\right]}$$

The number of reflections per unit length that the light travels in an optical waveguide.

Critical thickness of the film h=0.2$\frac{8}{}$ μm.

From Goos-Haenchen Analysis [26] the light ray penetrates (for a certain depth δ) into the confining layers 1 and 3, before it is reflected.

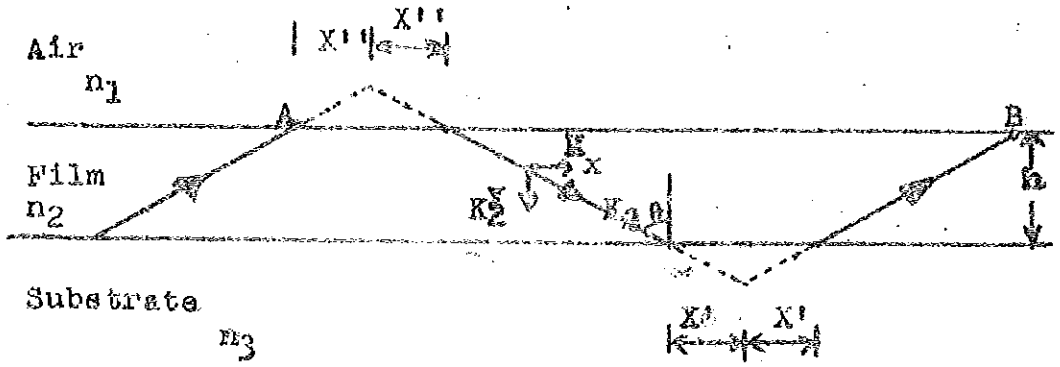

For TE modes, it is given that at the boundaries

$$X_i = \frac{1}{B_i} \tan\theta$$

At the film-substrate interface

$$X' = \frac{1}{B_3} \tan\theta = \frac{1}{K_0\left(n_{eff}^2 - n_3^2\right)^{1/2}} \times \frac{n_{eff}}{\left(n_2^2 - n_{eff}^2\right)^{1/2}}$$

Where $\sin\theta = \frac{K_x}{K_2} = \frac{K_0 n_{eff}}{K_0 n_2} = \frac{n_{eff}}{n_2}$

and $\cos\theta = \sqrt{1-\sin^2\theta} = \sqrt{1-\frac{n_{eff}^2}{n_2^2}}$

$\therefore \tan\theta = \frac{n_{eff}}{\sqrt{n_2^2 - n_{eff}^2}}$ and $X' = \frac{1}{K_0\sqrt{n_{eff}^2 - n_3^2}} \frac{n_{eff}}{\sqrt{n_2^2 - n_{3ff}^2}}$

At the air- film boundary

$$X'' = \frac{1}{B_1} \tan\theta = \frac{1}{K_0\left(n_{eff}^2 - n_1^2\right)^{1/2}} \cdot \frac{n_{eff}}{\left(n_2^2 - n_{eff}^2\right)^{1/2}}$$

Let ℓ = total distance travelled in X- direction from A to B.

$$\ell = 2X' + 2X'' + 2h \tan \Theta$$

Hence the number of reflection N

$$N = \frac{1 \text{ cm}}{\ell} = \frac{1754}{}.$$

Wehen we take

$n_1 = 1$, $n_2 = 1.6$, $n_3 = 1.5$, neff = 1.51.

References

1. P.K. Tien, Scientific American Vol. 230, No. 4, 1974.
2. M.C. Hamilton, D.A. Wille, W.J. Micelli Opt. Engin., Vol. 16, p. 475, 1977.
3 D. Mergerian, E.C. Malarkey, Microwave J. V. 23, p. 37, 1980.
4. M.E. Pedinoff, T.R. Ranganath, T.R. Joseph, J.Y. Lee. Proc edings of the NASA Conference on Optical Information Processing for Aerospace Applications, p. 173, 1981.
5. K.Aiki, M. Nakamura, J. Umeda, IEEE.J. QE-13, p. 597, 1977.
6. H.F. Taylor, IEEE J. V. 15, p. 210, 1979.
7. F. Koyama, S. Arai, T. Tanbun-EK, K. Kushimo, Y. Suematsu, Digest of Technical Papers, IEEE/OSA Topical Meeting o Integrated and Guidedwave optics, Asilomar p. WB-5, 19
8. Amnon Yariv, Scientific American V. 240, No. 1, 1979.
9. Max Born, in the book Principles of Optics.
10. P.K. Tien and R. Ulrich JOSA, V. 60, No. 10, p. 1325, 1970.
11. G.R. Fowled in the book Introduction to modern optics.(1975)
12. R. Shubert and J.H. Harris, JOSA. V. 61, No. 2, 1970.
13. L.Levi-Applied Optics, A Guide to optical system design v.1, 1968.
14. S. Sottini, V.Russo, G.C. Righini, JOSA, V. 69, No. 9, 1979.
15. L.Montagnino J.opt. Soc. Am. V. 58. p. 1667, 1968.
16. W.H. Southwell, JOSA V. 67, No. 8, 1977.

17. P.E/ Lagasse Digest of Technical Pepers Topical Meeting on Integrated and Guided-wave optics. 1982.

18. K.F. Eskin and I.I.Magdina Opt. & Spectr. V. 61, No. 1. p. 109, 1986.

19. V.I. Anikin and D.A. Leto v. opt. spectr. (U.S.S.R). 44(1), 1978.

20. R.C. Alferness, C.H. Joyner and L.L. Buhl.

21. R.G. Hunsperger in the book Integrated optics: Theory and Technology N.Y. 1982.

22. L.M. Brekhouskikh in the book waves in layered media, Acade Press Pub. N.Y. p. 462, 1960.

23. J.W. Goodman Introduction to Fourier Optics, Mc-Graw Hill, N.Y. p. 61, 1968.

24. E.W. Merchand, J.Opt. soc. Am. V. 60 No. 1. p. 1, 1970.

25. D.A. Letov, opt. spectrosc. (USSR), V. 45, No. 4, p. 705, 1978.

26. H. Kogelnik and H.P. Weber JOSA V 64, No. 2, p. 174, 1974.

Appendix IV

/ The method of the solution was kindly suggested by Dr.Mal'nev. /

The given integral has the form

$$I = \int_{\rho}^{1} \frac{\arcsin x}{\sqrt{x^2-\rho^2}}\,dx \qquad (4.1)$$

Let's introduce a new variable $Z = x/\rho$

$$I(\rho) = \int_{\rho}^{1} \frac{\arcsin}{\rho\sqrt{\left(\frac{x}{\rho}\right)^2-1}}\,dx =$$

$$= \int^{1/\rho} \frac{\arcsin Z}{\sqrt{Z^2-1}}dZ \qquad (4.2)$$

Simbolically the integral (4.2) can be written as

$$I(\rho) = \int_{1}^{\rho} f(\rho,Z)|dZ = F(\rho,Z)\Big|_{Z=\frac{1}{\rho}} - F(\rho,Z)\Big|_{Z=1}$$

$$= F(\rho,Z(\rho))\Big|_{Z=\frac{1}{\rho}} - F(\rho,Z)\Big|_{Z=1} \qquad (4.3)$$

Notice that Z becomes a constant in the last term, but $Z=Z(\rho)$ in the preceeding term. Differentiating eq(4.3) with respect to ρ

$$\frac{d\,I(\rho)}{d\rho} = \frac{d}{d\rho}\left(F(\rho,Z(\rho))\Big|_{Z=\frac{1}{\rho}}\right) - \frac{d}{d\rho}\left(F(\rho,Z)\Big|_{Z=1}\right)$$

$$= \frac{dF}{d\rho}\Big|_{Z=\frac{1}{\rho}} + \frac{\partial F}{\partial Z}\frac{dZ}{d\rho}\Big|_{Z=\frac{1}{\rho}} - \frac{dF}{d\rho}\Big|_{Z=1}$$

$$= \frac{dF}{d\rho}\Big|_{Z=\frac{1}{\rho}} - \frac{dF}{d\rho}\Big|_{Z=1} + \frac{\partial F}{\partial Z}\frac{dZ}{d\rho}\Big|_{Z=\frac{1}{\rho}}$$

$$\frac{dI(\rho)}{d\rho} = \frac{d(f(\rho,Z)dz)}{d\rho}\Big|_{Z=\frac{1}{\rho}} - \frac{d}{d\rho}\left(\int f(\rho,z)dz\right) + f(\rho,z)\frac{dz}{d\rho}\Big|_{Z=\frac{1}{\rho}}$$

$$= \int_1^{1/\rho} \frac{d}{d\rho}(f(\rho,z))dz - \int_1^{1/\rho} \frac{d}{d\rho}(f(\rho,z)dz + f(\rho,z)\frac{dz}{d\rho}\Big|_{z=\frac{1}{\rho}}$$

$$= \int_1^{1/\rho} \frac{d}{d\rho}(f(\rho,z))dz + f(\rho,z)\frac{dz}{d\rho}\Big|_{z=\frac{1}{\rho}}$$

$$= \int_1^{1/\rho} \frac{zdz}{\sqrt{z^2-1}\sqrt{1-\rho^2z^2}} + \frac{\arcsin 1\,(-\frac{1}{\rho^2})}{\sqrt{\frac{1}{\rho^2}-1}}$$

$$= \int_1^{1/\rho} \frac{zdz}{\sqrt{-\rho^2z^4+z^2+\rho^2z^2-1}} - \frac{\pi/2}{\rho\sqrt{1-\rho^2}}$$

$$= \frac{1}{2}\int_1^{1/\rho} \frac{d(z^2)}{\sqrt{-\rho^2z^4+(1+\rho^2)z^2-1}} - \frac{\pi/2}{\rho\sqrt{1-\rho^2}} \qquad (4.4)$$

Let's use the substitution $z^2 = t$ to evaluate the integral in eq.(4.4)

$$\frac{1}{2}\int_1^{1/\rho} \frac{d(z^2)}{\sqrt{-\rho^2z^4+(1+\rho^2)z^2-1}} = \frac{1}{2}\int_1^{1/\rho^2} \frac{dt}{\sqrt{-\rho^2t^2+(1+\rho^2)t-1}} \qquad (4.5)$$

From the table of indefinite integrals it is known (if $a<0$)

that

$$\int \frac{dx}{\sqrt{ax^2+bx+c}} = -\frac{1}{\sqrt{-a}} \arcsin \frac{2ax+b}{\sqrt{b^2-4ac}} \qquad (4.6)$$

Application of this result in formula (4.5) gives

$$\frac{1}{2}\int_1^{1/\rho^2} \frac{dt}{\sqrt{-\rho^2t^2+(1+\rho^2)t-1}} = \frac{1}{2}(-\frac{1}{\rho}) \arcsin \frac{-2\rho^2t+1+\rho^2}{1-\rho^2}\Big|_1^{1/\rho^2}$$

$$= -\frac{1}{2\rho}\left[\arcsin(-1)-\arcsin(+1)\right] = \frac{\pi}{2\rho} \qquad (4.7)$$

The result of eq.(4.7) can be achieved by Euler's substitution

if to take the integral under discussion in a form

$$\int_1^{1/\rho} \frac{zdz}{\sqrt{z^2-1}\sqrt{1-\rho^2z^2}} = \frac{1}{2}\int_1^{1/\rho^2} \frac{dt}{(t-1)(1-\rho^2t)} \qquad (4.8)$$

Euler's substitution is

$$\sqrt{(t-1)(1-\rho^2 t)} = \sqrt{(t-1)(\rho^2 t-1)(-1)} = y(t-1)$$

Squaring both sides

$$(t-1)\,(1-\rho^2 t) = y^2(t-1)^2$$

$$\text{or } y = \sqrt{\frac{1-\rho^2 t}{t-2}} \tag{4.9}$$

From eq.(4.9) we determine the new limits of the integral

if $t=1$, $y = \infty$

$t = 1/\rho^2$, $y = 0$

Again from eq. (4.9) we can express t as a function of y.

$$1-\rho^2 t = y^2(t-1)$$

$$-\rho^2 t - y^2 t = -y^2 - 1$$

$$t = \frac{1+y^2}{\rho^2+y^2}, \quad \frac{dt}{dy} = \frac{(\rho^2+y^2)2y-2y(1+y^2)}{(\rho^2+y^2)^2}$$

Using equations (4.10), (4.9) in (4.8).

$$\tfrac{1}{2}\int_1^{1/\rho^2} \frac{dt}{\sqrt{(t-1)(1-\rho^2 t)}} = \tfrac{1}{2}\int_\infty^0 \frac{2y(\rho^2-1)dy}{y(t-1)\,(\rho^2+y^2)^2}$$

$$\tfrac{1}{2}\int_1^{1/\rho^2} \frac{dt}{\sqrt{(t-1)(1-\rho^2 t)}} = \tfrac{1}{2}\int_\infty^0 \frac{2y(\rho^2-1)dy}{y\left(\frac{1+y^2}{\rho^2+y^2}-1\right)(\rho^2+y^2)^2}$$

$$= \int_0^\infty \frac{(1-\rho^2)dy}{(1+y^2-\rho^2-y^2)(\rho^2+y^2)^2}\,(y^2+\rho^2) = \int_0^\infty \frac{dy}{\rho^2+y^2}$$

$$= \frac{1}{\rho^2}\int_0^\infty \frac{dy}{1+y^2/\rho^2} = \frac{1}{\rho}\int_0^\infty \frac{d(y/\rho)}{1+y^2/\rho^2}$$

$$= \frac{1}{\rho}\arctan\frac{y}{\rho}\Big|_0^\infty = \frac{\pi}{2\rho} \tag{4.11}$$

Using results of eq.(4.11) or (4.7) in eq.(4.4) gives

$$\frac{dI(\rho)}{d\rho} = \frac{\Pi}{2\rho} - \frac{\Pi}{2\rho\sqrt{1-\rho^2}} = \frac{\Pi}{2}\left(\frac{1}{\rho} - \frac{1}{\rho\sqrt{1-\rho^2}}\right) \qquad (4.12)$$

In order to find the original integral eq.(4.1) we have to integrate eq.(4.12) with respect to ρ.

$$dI(\rho) = \frac{\Pi}{2}\left(\frac{1}{\rho} - \frac{1}{\rho\sqrt{1-\rho^2}}\right)d\rho$$

$$I(\rho) = \frac{\Pi}{2}\left\{\int \frac{1}{\rho}\,d\rho - \int \frac{d\rho}{\rho\sqrt{1-\rho^2}}\right\} \qquad (4.13)$$

Lets introduce a new variable $\alpha = \frac{1}{\rho}$ in eq.(4.13).

Thus $\rho = \frac{1}{\alpha}$, $d\rho = -\frac{1}{\alpha^2}d\alpha$

$$I(\alpha) = \frac{\Pi}{2}\left[-\int \frac{d\alpha}{\alpha} + \int \frac{d\alpha}{\alpha^2 \frac{1}{\alpha}\sqrt{1-\frac{1}{\alpha^2}}}\right]$$

$$= \frac{\Pi}{2}\left[\int \frac{d\alpha}{\sqrt{\alpha^2-1}} - \int \frac{d\alpha}{\alpha}\right]$$

$$= \frac{\Pi}{2}\left[\ln\left(\alpha+\sqrt{\alpha^2-1}\right) - \ln\alpha\right]$$

$$= \frac{\Pi}{2}\ln\frac{\alpha+\sqrt{\alpha^2-1}}{\alpha} = \frac{\Pi}{2}\ln\left(1+\frac{\sqrt{1/\rho^2-1}}{1/\rho}\right)$$

$$= \frac{\pi}{2}\ln\left(1+\sqrt{1+\rho^2}\right)$$

$$I(\rho) = \Pi\ln\sqrt{1+\sqrt{1+\rho^2}} \qquad (4.14)$$

Now finally let's substitute the result (4.14) in the equation for a spherically symmetric index distribution n(r) that gives a perfect image of an infinite object (where $\rho = r.n$)

$$n(r) = \exp\left(\frac{1}{\pi}\int_{\rho}^{1}\frac{\arcsin x}{\sqrt{x^2-\rho^2}}\,dx\right)$$

$$= \exp\left(\frac{1}{\pi}\times\pi\ln\sqrt{1+\sqrt{1-\rho^2}}\right)$$

$$= \sqrt{1+\sqrt{1-\rho^2}} = \sqrt{1+\sqrt{1-r^2n^2}} \qquad (4.15)$$

squaring both sides

$$n^2 = 1+\sqrt{1-r^2n^2}$$

$$n^2-1 = +\sqrt{1-r^2n^2}$$

Again squaring both sides

$$n^4-2n^2+1 = 1-r^2n^2$$

$$n^4-(2-r^2)n^2 = 0$$

$$n^2-(2-r^2) = 0$$

$$n^2 = 2-r^2$$

$$n = \sqrt{2-r}$$